REVIEW

Check for updates

Electrochemical CO_2 reduction with ionic liquids: review and evaluation†

Yangshuo Li, [iD]a Fangfang Li,a Aatto Laaksonen,abcde Chuan Wang,f Paul Cobden, [iD]f Per Boden,g Yanrong Liu,h Xiangping Zhang [iD]h and Xiaoyan Ji*a

The increasing CO_2 emission, as the chief culprit causing numerous environmental problems, could be addressed by the electrochemical CO_2 reduction (CO_2R) to the added-value carbon-based chemicals. Ionic liquids (ILs) as electrolytes and co-catalysts have been widely studied to promote CO_2R owing to their unique advantages. Among the potential products of CO_2R, those only containing one carbon atom, named C1 products, including CO, CH_3OH, CH_4, and syngas, are easier to achieve than others. In this study, we first summarized the research status on CO_2R to these C1 products, and then, the state-of-the-art experimental results were used to evaluate the economic potential and environmental impact. Considering the rapid development in CO_2R, future scenarios with better CO_2R performances were reasonably assumed to predict the future business for each product. Among the studied C1 products, the research focuses on CO, where satisfactory results have been achieved. The evaluation shows that producing CO *via* CO_2R is the only profitable route at present. CH_3OH and syngas of H_2/CO (1:1) as the targeted products can become profitable in the foreseen future. In addition, the life cycle assessment (LCA) was used to evaluate the environmental impact, showing that CO_2R to CH_4 is the most environmentally friendly pathway, followed by the syngas of H_2/CO (2:1) and CO, and the further improvement of the CO_2R performance can make all the studied C1 products more environmentally friendly. Overall, CO is the most promising product from both economic and environmental impact aspects.

Keywords: Electrochemical-CO_2-reduction; Ionic-liquids; C1-product; Economic-evaluation; Environmental-impact.

1. Introduction

On the one hand, the increasing anthropogenic CO_2 emissions due to the long and extensive burning of fossil fuels have caused severe environmental problems, such as the greenhouse effect leading to extreme weather events due to the rise of Earth's surface temperature.[1] On the other hand, CO_2 itself is an abundant carbon resource that can be converted to chemicals and fuels. Therefore, carbon capture and utilization *via* conversion (CCU) have become an important strategy to mitigate CO_2 emissions and produce

a Energy Engineering, Division of Energy Science, Luleå University of Technology, Luleå 97187, Sweden. E-mail: xiaoyan.ji@ltu.se

b Department of Materials and Environmental Chemistry, Arrhenius Laboratory, Stockholm University, 106 91 Stockholm, Sweden

c Centre of Advanced Research in Bionanoconjugates and Biopolymers, Petru Poni Institute of Macromolecular Chemistry, Aleea Grigore Ghica-Voda, 41A, 700487 Iasi, Romania

d State Key Laboratory of Materials-Oriented and Chemical Engineering, Nanjing Tech University, Nanjing, 210009, P. R. China

e University of Cagliari, Department of Chemical and Geological Sciences, Campus Monserrato, SS 554 bivio per Sestu, 09042, Monserrato, Italy

f Metallurgy Department, Swerim AB, 97125, Luleå, Sweden

g SMA Mineral AB, 68227, Filipstad, Sweden

h CAS Key Laboratory of Green Process and Engineering, Beijing Key Laboratory of Ionic Liquids Clean Process, State Key Laboratory of Multiphase Complex Systems, Institute of Process Engineering, Chinese Academy of Sciences, Beijing 100190, China

† Electronic supplementary information (ESI) available. See DOI: https://doi.org/10.1039/d2im00055e

Yangshuo Li received her BE degree in Chemistry from Henan Normal University in 2018, and ME degree in Physical Chemistry from Henan Normal University in 2021. She is currently a Ph.D. candidate in Energy Science under the supervision of Prof. Xiaoyan Ji at Luleå University of Technology. Her doctoral research focuses on the electrochemical CO_2 reduction to CO with ionic liquids as electrolytes.

Yangshuo Li

carbon-based chemicals and fuels.[2–4] Several methods have been proposed to convert CO_2, including thermal,[5] chemical,[6] and bio-conversion[7] as well as electrocatalytic,[8–10] photocatalytic,[11] and photoelectric[12] conversions and co-conversions. Among them, electrochemical CO_2 reduction (CO_2R) is among the most promising owing to the mild reaction conditions, as well as easy and flexible controllability. Also, its driving force, electricity, can be potentially integrated with renewable energy sources, for example, solar and wind power.[13–15]

The performance of CO_2R is mainly characterized by the faradaic efficiency (FE), current density, and cell voltage, reflecting product selectivity, reaction rate, and energy usage.[16] Therefore, higher FE and current density as well as lower cell voltage are being pursued in the performance of CO_2R, where the suitable electrocatalyst, electrolyte, electrolyzer, and applied potential, as well as reaction temperature and pressure, can all contribute to the performance. Currently, the research on electrocatalysts has focused on noble metals (Au, Ag, Pt),[17–22] transition metal disulfide compounds (MoS_2, $MoSe_2$, WS_2),[23–26] metal organic frames,[27] graphene-based synthetic materials,[28–30] and molecular and single-atom catalysts[31,32] for their desirable catalytic performances.[33] While in CO_2R, the electrolyte not only enriches the dissolved CO_2 (as the carbon source) but also provides protons for the reduction, so that their concentration, pH, and buffer capacity can affect the local reaction conditions, thereby a variety of products.[10,34–36] Thus, it is desirable to have an electrolyte having the ability to dissolve CO_2 and then stabilize it as the reaction intermediate. Previously, the aqueous solutions of sodium and potassium salts have been widely used as electrolytes, but their solubility of CO_2 is limited.[33,37–40] Recently, it has been discovered that ionic liquids (ILs) can greatly promote the performance of CO_2R because IL is a powerful CO_2 absorbent, and additionally, ILs can also activate CO_2 to facilitate the further conversion (co-catalyst).[41–45] ILs themselves are electrolytes, which can also be readily mixed with other electrolytes. Besides, ILs, with their tunable structures and properties, wide electrochemical windows, and high electrical conductivities, can provide a lower overpotential, a higher current density, and improved product selectivity for CO_2R.[46–49] Significantly, ILs can effectively inhibit the hydrogen evolution reaction (HER), which is a competitive reaction with CO_2R.

Developing IL-based CO_2R has been studied. It was found that, when ILs were immobilized into the cathode catalyst, the cell operating current was increased by a factor of two or more, and FE was enhanced by 20–30%, indicating that ILs could effectively promote CO_2R.[42] Rosen et al.[50] were the first to report that the use of 1-ethyl-3-methylimidazolium tetrafluoroborate ([EMIM][BF_4]) increased the selectivity for CO and lowered the overpotential. Since then, developing ILs as electrolytes have been intensively studied, and their efficiency has grown tremendously. Kumar et al.[51] performed CO_2R to CO in the [BMIM][BF_4] electrolyte, showing an extremely low overpotential of 0.17 V over the metal-free carbon nanofiber electrode. Choi et al.[52] demonstrated that the addition of [EMIM][BF_4] into an aprotic electrolyte could reduce the overpotential and enhance the kinetics of electron transfer for CO_2R, and the turnover frequency (TOF) in the IL-based systems was 4 times higher than without ILs. Min et al.[53] reported that the current density of syngas could reach up to 644.7 mA cm^{-2} in the gas diffusion electrode (GDE) electrolyzer with the imidazolium-based ILs as the electrolytes. Furthermore, the product of CO_2R was changed

Fangfang Li

Fangfang Li received her BE degree in Chemistry from Zhengzhou University in 2016, and ME degree in Chemical Engineering from University of Chinese Academy of Sciences in 2019. She is currently a Ph.D. candidate in energy science under the supervision of Prof. Xiaoyan Ji at Luleå University of Technology. Her doctoral research focuses on the electrochemical CO_2 reduction to CH_3OH with ionic liquids as electrolytes.

Xiaoyan Ji

Xiaoyan Ji got her Ph.D. degree in Chemical Engineering in 2000 with more than 25 years of experience in research and development in the area of Chemical Engineering and Energy Engineering. She has taken part in projects in research groups in China, Sweden, Germany, and the US. Her research work is from theoretical modeling to technology development, as well as process simulation and evaluation.

Xiaoyan Ji started working at the division of Energy Science, Lulea University of Technology, in 2008. She created a research group on "Advanced fluid materials for energy applications", where CO_2 capture/separation, CO_2 electrochemical conversion, advanced electrolytes for batteries, and lignin conversion coupling H_2 production via electrochemical process are the focus.

Review

View Article Online

Industrial Chemistry & Materials

Open Access Article. Published on 01 2023. Downloaded on 6/9/2025 08:24:07. This article is licensed under a Creative Commons Attribution-NonCommercial 3.0 Unported Licence.

into CO from syngas by replacing the C2–H of the imidazolium cation with methyl, and the current density could reach up to 528.3 mA cm^{-2}, which has already achieved the industrial standard, indicating that the IL-based electrolytes are efficient in GDE. All these studies indicate that ILs can play an important role in CO_2R.

Among the potential products that can be obtained from CO_2R with ILs, the ones containing just one carbon atom, named C1 products, including CO, CH_3OH, CH_4, or syngas, are easier to achieve. Much research work has already been conducted and even summarized in review articles.[46,54–57] However, we feel that the recent studies now lead to a rapidly improving performance call for a fresh update. Also, such constant improvements in technological development attract great attention and interest toward novel implementations. To understand the economic feasibility of CO_2R with ILs as electrolytes, Chang et al.[58] evaluated CO_2R to CO, pointing out that it could be competitive with fossil fuels when the current density reached 200 mA cm^{-2} at the condition of 99% FE. Rumayor et al.[59] analyzed the competitiveness of CHOOH generation from CO_2R in comparison to traditional methods, concluding that the CO_2R pathway was more economically feasible. On the other hand, Jouny et al.[60] evaluated the commercial value for CO_2R without limiting the types of systems, including non-IL-based electrolytes, and products, including syngas, CO, CHOOH, CH_3OH, CH_4, C_2H_4, C_2H_5OH, and n-C_3H_8O by calculating the end-of-life net present value (NPV) using the state-of-the-art indicators in 2018. However, IL, as an efficient and green solvent that can replace toxic organic solvents and conventional aqueous carbonate solutions with limited CO_2 solubility, has always been sufficiently interested and concerned as novel electrolytes for CO_2R, and the research on IL-based electrolytes is extensively booming in recent years due to the unique advantages of ILs in CO_2R. To the best of our knowledge, no work has been conducted to discuss and systematically compare the economic benefits of different C1 products focusing on IL-based electrolyte systems, as well as analyzing environmental impacts.

Therefore, in this work, to evaluate and compare the economic potential and environmental impact of CO_2R to C1 with ILs as electrolytes, a thorough literature survey was conducted to update the research progress and provide state-of-the-art research achievements for different target C1 products, including CO, syngas, CH_4, and CH_3OH, which was performed in H-cell. Subsequently, the economic performance was evaluated, and the environmental impact was analyzed based on the state-of-the-art research achievement. Considering the rapid development in CO_2R, several future scenarios with improved FE and current density, as well as decreased cell voltage for each target C1 product, were created, and their performances from both economic and environmental aspects were predicted. Additionally, a sensitivity analysis was conducted to provide a comprehensive understanding of how the main parameters would affect TPC for each product. Finally, the traditional and IL-based electrolytes were compared from economic and environmental aspects.
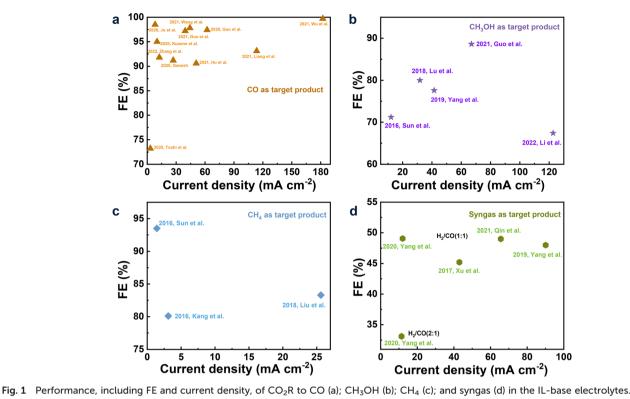
2. IL-based electrochemical CO_2 reduction to C1 products

In general, aqueous solutions containing carbonate sodium and potassium salts are used as the electrolyte for CO_2R, but the product selectivity and current density are often unsatisfactory. To address these problems, IL-based electrolytes can be used to improve the absorption capacity of CO_2 and stabilize the intermediate, and reconstruct the electrode interface.[61–63] Herein, the achievements of CO_2R to CO, CH_3OH, CH_4, and syngas in IL-based electrolytes are summarized in the following subsections, and the best performance for each target product was identified for further evaluation.

2.1. CO as the target product

The electrochemical conversion of CO_2 to CO is the most promising one among the various CO_2R pathways due to the lower electron demand ($2e^-$) for the formation of CO and the pivotal role of CO in the industry as the primary ingredient for the synthesis of hydrocarbons and alcohols.[64–66] Recently, relevant research is growing fast, and previous important research work has been summarized in review articles published in the past few years.[67] Therefore, we focused only on the latest research, reported mainly since 2020, as summarized in Fig. 1a.

For the IL-based CO_2R to CO, Liang et al.[68] reported that the FE of CO and current density could be up to 93.1% and 122.0 mA cm^{-2}, respectively, in the 1-butyl-3-methylimidazolium hexafluorophosphate ([BMIM][PF$_6$])/acetonitrile (MeCN) electrolyte. In the work of Oguma and Azumi,[69] 1-ethyl-3-methylimidazolium ethyl sulfate ([EMIM][EtSO$_4$]) was added into the 0.1 mol dm^{-3} K_2CO_3 aqueous solution for CO_2R on the Ag electrode, and observable improvements in the FE of CO and current density were obtained, owing to the high complexation ability of EMIM with CO_2 that was intensively adsorbed on the electrode surface. Guo et al.[70] studied CO_2R in 0.5 mol L^{-1} (M) [BMIM][PF$_6$]/MeCN on the Cu–Co bimetallic electrode, and the FE of CO and the current density could reach 97.4% and 62.1 mA cm^{-2}, respectively. Zhang et al.[71] designed a catalyst with ZIF-8 films on Zn foils (ZIF-8/Zn) to promote CO_2R, and FE$_{CO}$ of 91.8% along with the current density of 12.6 mA cm^{-2} was obtained at −1.9 V in the electrolyte with (30 wt% [BMIM][PF$_6$] + 65 wt% MeCN + 5 wt% water). Kunene and co-workers[72] explored the CO_2R to CO in the MeCN/100 mmol L^{-1} (mM) tetrabutylammonium hexafluorophosphate ([TBA][PF$_6$]) electrolyte with 1-butyl-3-methylimidazolium trifluoromethanesulfonate ([BMIM][OTf]) as the additive on the soldering alloy $Bi_{50}Sn_{22}Pb_{28}$ as the anode, where the influences of [BMIM][Otf] concentrations (50, 100, and 200 mM) and the applied potentials (−1.85, −1.95, and −2.05 V) on CO_2R were investigated. The result showed that the FE of 95% and current density of 10.2 mA cm^{-2} were obtained when the concentration of [BMIM][Otf] was 100 mM at −2.05

© 2023 The Author(s). Co-published by the Institute of Process Engineering, Chinese Academy of Sciences and the Royal Society of Chemistry

Fig. 1 Performance, including FE and current density, of CO_2R to CO (a); CH_3OH (b); CH_4 (c); and syngas (d) in the IL-base electrolytes.

V. To make the CO_2R to CO more economical with ILs as the electrolytes, Ganesh[73] synthesized the low-cost highly pure 1-butyl-3-methylimidazolium tetrafluoroborate ([BMIM] [BF$_4$]) using the inexpensively accessible raw materials (1-bromobutane (BB) and 1-methylimidazole (MI)). The 20 mM synthesized [BMIM][BF$_4$] was mixed with 0.1 M [TBA] [PF$_6$] and MeCN and then used as the electrolyte to perform CO_2R on the Sn and $MoSi_2$ electrodes, obtaining FE of 91.2% and the current density of 27 mA cm^{-2} at 622 mV potential.

The linear CO_2 being very thermodynamically stable and kinetically inert is difficult to be reduced, and the formation of CO$^{·-}$ radical in the first-step one-electron reduction of CO_2 is the major obstacle, which requires a high potential.[74] It was reported that the formation of the CO_2-imidazolium intermediate compound could help to reduce the overpotential of CO_2R. Ju and co-workers[75] discovered that the imidazolium ILs could be adsorbed on the electrode and form a film layer during CO_2R, which can help CO_2 to contact the catalyst and stabilize the generated $CO_2^{·-}$ after the CO molecule obtains an electron according to the comparison of six imidazolium-ILs, consisting of the same anion [BF$_4$]$^-$ and different cations ([EMIM]$^+$, [BMIM]$^+$, 1-hexyl-3-methyl-imidazolium ([HMIM]$^+$), 1-methyl-3-octyl-imidazolium ([OMIM]$^+$) and 1,3-dimethyl-imidazolium ([DMIM]$^+$)), with [TBA][BF$_4$] in propylene-carbonate (PC) as the electrolytes. Among them, [BMIM][BF$_4$] was identified as the most efficient electrolyte, which may be attributed to its suitable chain length at the N1-position of the imidazolium cation. Hu *et al.*[76] found that, in the system of

N-octyltrimethyl ammonium 1,2,4-triazole ([N$_{1118}$][TRIZ])/ MeCN electrolyte, the linear CO_2 molecule could change into a bend because the extra electron was filled in the lowest unoccupied molecular orbital (LUMO) from [TRIZ]$^-$. The formation of the [TRIZ–CO_2] complex was emphasized and demonstrated *via* Fourier transform infrared (FTIR), which could result in the high solubility of CO_2 and low energy barrier for CO_2 activation.

To confirm the role of imidazolium-2-carboxylate species, Ratschmeier and Braunschweig[77] detected the produced CO molecule adsorbed on the Pt electrode in the 1-butyl-3-methylimidazolium bis(trifluoromethylsulfonyl)imide ([BMIM][NTf$_2$]) with 0.5 M H_2O electrolyte *via* the *in situ* vibrational sum-frequency generation (SFG). Also, the *in operando* Fourier transform infrared reflection absorption spectroscopy (FT-IRAS) was used to determine the formation of imidazolium-2-carboxylic acid species. The investigation revealed that the mechanism strongly depended on the types of ILs. For [BMIM][NTf$_2$], providing an active C2 position of the imidazolium ring, the [BMIM]-2-carboxylic acid species could be generated through the carbene intermediate. While for 1-butyl-2,3-dimethylimidazolium bis(trifluoromethylsulfonyl)imide ([BMMIM][NTf$_2$]) with protected C2 position by the methyl group and 1-butyl-1-methyl pyrrolidinium bis(trifluoromethylsulfonyl)imide ([BMPyrr][NTf$_2$]) without the active C2 position (their structures were shown in Fig. 2), when 0.5 M H_2O was used as the electrolyte, the stabilization of $CO_2^{·-}$ was attributed to the formation of bicarbonate and the Coulomb interactions between $CO_2^{·-}$ and the IL-cations. Meanwhile,

© 2023 The Author(s). Co-published by the Institute of Process Engineering, Chinese Academy of Sciences and the Royal Society of Chemistry

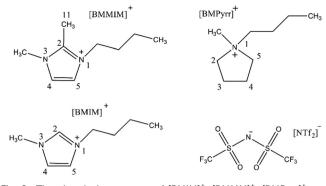*Ind. Chem. Mater.*, 2023, **1**, 410–430 | **413**

Fig. 2 The chemical structures of [BMIM]$^+$, [BMMM]$^+$, [BMPyrr]$^+$, and [NTf$_2$]$^-$.[77] Copyright 2021 American Chemical Society.

the anion can also effectively facilitate CO$_2$R to CO. For example, Hu and co-workers[76] developed a novel IL [N$_{1118}$][TRIZ] and used it as the electrolyte to explore the effect on CO$_2$R, where the electrochemical methods, FTIR spectroscopy, and the density functional theory (DFT) were combined to analyze the mechanism. It showed that the 1,2,4-triazole ([TRIZ]) anion was equally effective for facilitating CO$_2$R to CO on the Ag electrode.

To overcome the high viscosity of ILs, adding H$_2$O or organic solvent is an efficient way, and their content plays an important role. In the work of Wang et al.,[78] CO$_2$R to CO was explored with various contents of [BMIM][PF$_6$] and H$_2$O in the MeCN electrolyte, where a series of porous zinc oxide nanosheets grafted with the hydroxyl groups on the carbon paper substrates were used as the catalyst. They found that the current density first raised and then dropped with increasing H$_2$O concentrations. This observation was caused by the appropriate electrostatic attraction between the anions and cations, availing the ion movement and charge transport and thereby promoting CO$_2$R. In this work, the best performance was obtained at a low overpotential of 340 mV when 5 wt% H$_2$O was added into 30 wt% [BMIM][PF$_6$]-based electrolytes, where the addition of H$_2$O might increase the electrolyte conductivity and the CO$_2$ solubility by changing the microstructure of the electrolyte. Similarly, Hu et al.[76] explored the influence of the H$_2$O contents on the current density, drawing analogical conclusions. With increasing water content from 0 to 7.5 wt%, the onset potential of CO$_2$R was changed from −1.93 to −1.75 V vs. Ag/Ag$^+$, indicating that the addition of water reduced the initial reduction energy barrier.

Apart from the co-catalysis concept of ILs as the electrolyte, the coupling of electrocatalyst and IL-based electrolyte can be another important accelerant for CO$_2$R. To further provide a comprehensive insight into the synergistic effect of catalysts and IL-based electrolytes, Rudnev and co-workers[79] explored the performance of thirteen catalyst materials, including Pt, Ag, Bi, Sn, Mo, Zn, Pd, Cu, Au, Pb, Ni, Fe, and glassy carbon (GC), in three IL-based electrolytes ([BMIM][BF$_4$], [BMIM][NTf$_2$] and [BMPyrr][NTf$_2$]). It was found that the co-catalyst effect required balanced interactions

between the IL and the electrode surface, depending on the chemical properties of both the IL and catalyst material. Only the proper combination of ILs and electrode materials could enhance the performance of CO$_2$R. Besides, IL-anions significantly influenced the CO$_2$R peak current density in the order of [BMIM][BF$_4$] ≤ [BMIM][NTf$_2$] ≪ [BMPyrr][NTf$_2$], being consistent with the decreasing trend of their viscosities. This observation indicates that low viscosity leads to a high diffusion rate and then a high current density. Among their studied cases, the best performance (99.7% FE of CO) was obtained at −1.84 V when Ag was used as the electrode in the [BMIM][BF$_4$] electrolyte. Zeng et al.[80] also found that the combination of a nanoporous Au film electrode with [EMIM][BF$_4$]/H$_2$O as the electrolyte could efficiently perform electrocatalytic CO$_2$ to CO with high selectivity of 92.5% at a low overpotential of 440 mV. In this work, the CO$_2$ reduction rate was strongly affected by the transport rate of CO$_2$ within the nanopores of the Au film. The adsorption of [EMIM][BF$_4$] on the nanopore, confirmed by X-ray photoelectron spectroscopy (XPS), led to the high solubility of CO$_2$, improving the driving force in the mass transfer of CO$_2$ and thereby promoting CO$_2$ conversion. They also found that the performance of CO$_2$R in [EMIM][BF$_4$]/H$_2$O was superior compared to that in 1 M NaHCO$_3$ aqueous electrolyte, indicating the important role of IL.

Additionally, the catalyst itself is of importance in CO$_2$R. The research group of Han[81] conducted several studies on the catalysts. They found that the catalyst of the atomic anchored on the N-doped carbon (In$_A$/NC) could significantly promote CO$_2$R to CO in 0.5 M [BMIM][PF$_6$]/MeCN. As a result, the FE$_{CO}$ of 97.2%, a total current density of 39.4 mA cm^{-2}, and a TOF of 40 000 h^{-1} were obtained. Comparatively, FE$_{CO}$ and current density decreased to 53.3% and 0.9 mA cm^{-2}, respectively, when the electrolyte was replaced by 0.5 M KHCO$_3$ aqueous solution, also indicating the indispensable role of [BMIM][PF$_6$]. Later, Han's group[82] further improved the performance greatly by synthesizing a novel Cd single-atom catalyst (SACs) CdN$_4$S$_1$/CN, where 0.5 M [BMIM][PF$_6$]/MeCN was used as the electrolyte. The FE of CO could reach up to 99.7% along with the high current density of 182.2 mA cm^{-2} and the TOF of 73 000 h^{-1} at a low overpotential of 0.6 V. This is the most outstanding performance of CO$_2$R to CO in the H-type electrolysis cell so far. During this process, both the introduction of an axial coordination structure to the Cd SACs and the formation of [BMIM–CO$_2$]$^+$ in [BMIM][PF$_6$]/MeCN electrolyte could reduce the reaction barrier of CO$_2$R and suppress the competitive HER in the aprotic solvent.

2.2. CH$_3$OH as the target product

CH$_3$OH as the important platform molecule with high energy density can be converted to different chemicals and fuels.[35,83] The formation of one CH$_3$OH via CO$_2$R needs a transfer of six electrons (6e$^-$), making it more difficult to perform the reduction compared to CO$_2$R to CO.[56,57] Only a few related articles from Han's group reported improved

performance by designing and synthesizing efficient electrocatalysts in the IL-based electrolytes. These achievements are summarized in Fig. 1b.

Initially, Sun et al.[84] searched for efficient IL-based electrolytes among [BMIM][BF$_4$], [BMIM][PF$_6$], [BMIM][ClO$_4$], and [BMIM][NTf$_2$] in MeCN for electrocatalytic CO$_2$ conversion to CH$_3$OH over a Mo–Bi bimetallic chalcogenide on the carbon paper (CP) (Mo–Bi BMC/CP) electrocatalyst. As a result, the highest selectivity of CH$_3$OH was obtained with an FE of 71.2% and a current density of 12.1 mA cm^{-2} at −0.7 V (vs. the standard hydrogen electrode (SHE)) when [BMIM][BF$_4$] was the supporting electrolyte. On the contrary, CH$_3$OH was not detected in the tetrabutylammonium/ tetraethylammonium salts as the supporting electrolytes, suggesting the important role of ILs in the electrolyte. Additionally, different concentrations of [BMIM][BF$_4$] led to different FEs of CH$_3$OH and current density, further indicating the vital role of the IL in CO$_2$R. Similarly, Yang et al.[85] reported that [BMIM][BF$_4$] was the most efficient supporting electrolyte in the MeCN/H$_2$O solution for CO$_2$R to CH$_3$OH among the [BMIM]-based ILs with various anions (PF$_6^-$, NTf$_2^-$, OAC$^-$, NO$_3^-$, and ClO$_4^-$). Over the Cu$_{1.63}$Se electrode, the highest FE of CH$_3$OH and current density were 77.6% and 41.5 mA cm^{-2}, respectively.

Hereafter, Han's group further explored the electrocatalytic CO$_2$ conversion to CH$_3$OH in the [BMIM][BF$_4$] aqueous solution by designing and synthesizing efficient electrocatalysts. Lu et al.[86] synthesized a kind of bimetallic catalyst of Pd$_{83}$Cu$_{17}$ on CP as the electrode, which successfully enhanced the FE of CH$_3$OH and current density up to 80.0% and 31.8 mA cm^{-2}, respectively. Guo et al.[87] designed the atomically dispersed Sn site anchored on the defective CuO catalysts (Sn$_1$/V$_O$–CuO) with high conductivity in the [BMIM][BF$_4$]/H$_2$O electrolyte. The high selectivity of CH$_3$OH (FE of 88.6%) and current density (67.0 mA cm^{-2}) were obtained. In the work of Li et al.,[88] the current density surpassed 100 mA cm^{-2} for the first time with a value of 122.7 mA cm^{-2} by developing the Ag, S–Cu$_2$O/Cu electrocatalyst combined with [BMIM][BF$_4$]/H$_2$O as the electrolyte. During this process, the S anion could regulate the morphology and electron structure of the electrocatalyst, making it more efficient for CO$_2$R to CH$_3$OH, and, at the same time, the Ag cation could suppress the competing HER. The synergistic effect of the Ag and S heteroatoms and the Cu$_2$O/Cu host greatly contributed to the dramatic enhancement of the current density.

Sun et al.[84] studied CO$_2$R to CH$_3$OH using Mo–Bi BMC as the electrocatalyst in the [BMIM][BF$_4$]/H$_2$O electrolyte. They proposed that, in this system, firstly, the [BMIM–CO$_2$]$^+$ complex was quickly formed, reducing the reaction barrier. Furthermore, the synergistic effect of Mo and Bi atoms in Mo–Bi BCM/CP electrocatalyst greatly promoted the CO$_2$ reduction to CH$_3$OH. The Bi sites favored the formation of CO, and the Mo sites were for the generation of H$_2$, conducive to the further hydrogenation of CO to form CH$_3$-OH. By using Sn$_1$/V$_O$–CuO as the catalyst, Guo et al.[87] found

that the formation of Lewis acid–base interaction between the Sn single atom and the oxygen vacancy of CuO reduced the energy barrier for the dissociation of *COOH and conversion to *CO, which was confirmed via in situ X-ray absorption (XAS) spectra, in situ Raman spectra, and DFT. Subsequently, the formed *CO free radical was combined with Cu to generate *CHO, and the moderate binding energy of *CHO with the electrocatalysts promoted the production of *OCH$_2$ and further conversion to CH$_3$OH.

2.3. CH$_4$ as the target product

CH$_4$ is more difficult to produce via CO$_2$R compared to the other C1 products due to the high C–H bond energy (434 kJ mol^{-1}) and the 8e$^-$-transfer demand.[33,40,89–93] Therefore, it is a challenge to achieve high FE and current density. To the best of our knowledge, only three articles have reported satisfactory FE and current density in the IL-based electrolytes, as summarized in Fig. 1c.

Kang et al.[94] deposited Zn–1,3,5-benzenetricarboxylic acid metal–organic frameworks on carbon paper (Zn–BTC-MOFs/CP) as the electrocatalyst, and relatively high product selectivity (FE of 80.1%) and current density (3.1 mA cm^{-2}) in the pure [BMIM][BF$_4$] electrolyte at a low overpotential of 0.25 V were obtained. In this work, the combinations of different catalysts (Au, Ag, Pt, Fe, Zn) and electrolytes ([TBA][BF$_4$]/dimethylformamide (DMF), [TBA][PF$_6$]/MeCN, [BMIM][BF$_4$]/MeCN) were conducted, and the desired performance was attributed to the optimal compatibility between Zn–BTC-MOFs/CP and [BMIM][BF$_4$] as Zn–BTC-MOFs/CP was synthesized in the imidazolium-based ILs.

Sun et al.[95] reported an efficient catalyst, the metal-free electrode N-doped graphene-like materials (NGMs), for CO$_2$R to CH$_4$ in the [BMIM][BF$_4$]/H$_2$O electrolyte. It was found that FE was improved from 20.8 to 93.5% by increasing the content of the doped N from 1.8 to 4.8%, implying the vital importance of the active-doped N for the selective production of CH$_4$. A possible pathway (shown in Fig. 3) was proposed as follows: (1) CO$_2$$^{\cdot-}$ was firstly generated via CO$_2$ adsorbed on the active N sites of the electrode. (2) CO$_2$$^{\cdot-}$ was coupled with the CO$_2$ molecule dissolved in the electrolyte and then reduced to CO$_2$–CO$_2$$^{\cdot-}$. (3) after obtaining the second electron,

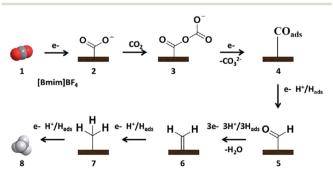**Fig. 3** Mechanism schematic diagram of CO$_2$ reduction to CH$_4$ at the NGM/CP electrode.[95] Copyright 2016 Royal Society of Chemistry.

© 2023 The Author(s). Co-published by the Institute of Process Engineering, Chinese Academy of Sciences and the Royal Society of Chemistry

Ind. Chem. Mater., 2023, 1, 410–430 | 415

the adsorbed CO was formed, i.e., CO_{ads}. (4) The formed CO_{ads} was converted to CHO_{ads} by accepting the proton. (5) the formed CHO_{ads} was further transformed to CH_4 after obtaining six electrons and protons. During this pathway, the strong interaction between CO_{ads} and electrons favored the hydrogenation of CO_{ads} to generate CHO_{ads}, an important intermediate of CO_2R to CH_4. On the other hand, [BMIM][BF_4]/H_2O as the electrolyte improved the solubility of CO_2, driving the transformation of CO_2 to $CO_2{}^{\cdot-}$.

In the same electrolyte, [BMIM][BF_4]/H_2O, by using $MoTe_2$ nanoflakes as the catalyst, Liu et al.[96] greatly improved the current density to 25.6 mA cm^{-2} along with the FE of 83%. Considering both the current density and FE of CH_4, the performance in this work was the best. Here, the $MoTe_2$ nanosheets provided more active sites and stronger adsorption capacity of CO_2 compared to the bulk materials, being beneficial for the CO_2 conversion, and the Tafel slope was very close to the theoretical value (68 mV dec^{-1}), indicating the ultrathin $MoTe_2$ to be an ideal catalyst. Additionally, the DFT calculations also suggested that the interaction between the $MoTe_2$ nanosheets and CO_2 molecules might be formed during CO_2R through the formation of intermediates.

2.4. Syngas as the target product

Syngas compositing of H_2 and CO, as an important feedstock in industry, is mainly derived from coal or natural gas, which are non-renewable resources.[97–99] CO_2R potentially provided a more energy-efficient method to produce syngas with different ratios by adjusting the reaction environment, including the electrolyte and catalyst.[100–106] Among them, H_2/CO with a ratio of 1:1, i.e., H_2/CO (1:1) is suitable for the Fischer–Tropsch hydrocarbon synthesis, while H_2/CO (2:1) can be used to synthesize formaldehyde via hydroformylation.[107–111] Herein, H_2/CO (1:1) and H_2/CO (2:1) were mainly discussed. The related available results are summarized in Fig. 1d.

The structures and properties of the catalysts greatly affect the ratio of syngas. Xu et al.[112] compared the efficiency of CO_2R to syngas by using the MoSeS alloy as well as the $MoSe_2$ and MoS_2 monolayers in the [EMIM][BF_4]/H_2O electrolyte. The MoSeS alloy monolayer exhibited the best catalytic effect, leading to the current density of 43 mA cm^{-2} along with the FE for CO of 45.2% at −1.15 V vs. the reversible hydrogen electrode (RHE). For comparison, the FE of CO for the MoS_2 and $MoSe_2$ catalysts was 16.6% and 30.5%, respectively. The high catalytic activities of the MoSeS alloy monolayer were attributed to its strong absorption ability of CO_2, high intrinsic conductivity, and low charge transfer resistance. Moreover, the desorption of CO* from the electrode was also an important influencing factor, and the MoSeS alloy monolayer exhibited low CO onset desorption temperature.

As reported, the synergistic effect of Au and Ni could be in favor of syngas generation under suitable conditions.[113–115] Inspired by this, Yang et al.[116] designed a kind of catalyst where the Au nanowires (Au NWs) were grown on the porous nickel

foam. They found that the porous nickel foam was mainly responsible for the electrocatalytic HER, while the Au NWs with large active surface areas and abundant edge sites were beneficial to the CO_2 conversion to CO. The longer and thinner the Au NW was, the higher selectivity of CO was obtained. On the contrary, when Au NWs were grown tightly on the nickel foam, the active sites would be covered, reducing the selectivity of CO and the overall catalytic performance.

Apart from the catalyst, the ratio of syngas also strongly depends on the applied potential and electrolytes. Yang et al.[117] synthesized a nanoflower-like catalyst γ-In_2Se_3 (F-γ-In_2Se_3/CP) for CO_2R in different IL-based electrolytes. Within the applied potential (−1.8 to 2.3 V), the ratio of H_2/CO was changed from 1:24 to 3:1. For the electrolyte with ([BMIM][PF_6], H_2O, and MeCN), upon increasing the [BMIM][PF_6] content from 5 to 70 wt%, the ratio of H_2/CO was changed from 1:24 to 16:9; upon increasing the H_2O content from 0 to 20 wt%, the ratio was varied from 1:24 to 3:2. Significantly, H_2/CO (1:1) was obtained with a current density of 90.1 mA cm^{-2} at the applied potential of −2.3 V in the electrolyte composed of (30 wt% [BMIM][PF_6] + 65 wt% MeCN + 5 wt% H_2O).

Similarly, Yang and co-workers[116] showed that the addition of H_2O into the electrolyte composed of [TBA]Br and DMF would greatly affect the ratio of syngas. This can be explained as follows. Without the addition of water, DMF could be oxidized to reduce protons in the anode chamber, thereby producing abundant H_2. After the addition of H_2O, the oxygenolysis of DMF could be suppressed, stabilizing the DMF. Besides, the addition of H_2O could also generate proton-coupled electron transfer (PCET) in favor of CO_2 activation, and enhance HER, which would have a great influence on the ratio of H_2/CO. The applied potential was also found to take an important role. H_2/CO (2:1) and H_2/CO (1:1) were obtained at −1.6 and −1.8 V, respectively, when the concentration of H_2O was 1 M. Qin et al.[118] also tuned the ratio of H_2/CO from 0.15:1 to 4:1 by controlling the applied potential in the [BMIM][PF_6]/MeCN electrolyte, where H_2/CO (1:1) was obtained with the current density of 65.6 mA cm^{-2} at −1.395 V vs. RHE.

2.5. Identification of the state-of-the-art research results

According to the reviews, when CO, CH_4, and syngas were chosen as the target products, their state-of-the-art research results can be identified according to their FE and current density. The corresponding results, together with the cell voltages, are listed in Table 1. While for CO_2R to CH_3OH, there were two potential cases, of which one is with an FE of 88.6% along with a current density of 67.0 mA cm^{-2}, the other showed a current density of 122.7 mA cm^{-2} along with an FE of 67.4%. Thus, a preliminary study on economic benefit was conducted (the detailed comparison can be found in the ESI†), showing the case with the FE of 88.6% along with the current density of 67.0 mA cm^{-2} as included in Table 1 was more promising and thus was chosen for further study.

According to the study conducted, the recent research is more on CO, followed by methanol, syngas, and methane

View Article Online

Industrial Chemistry & Materials **Review**

Open Access Article. Published on 01 2023. Downloaded on 6/9/2025 08:24:07. This article is licensed under a Creative Commons Attribution-NonCommercial 3.0 Unported Licence.

Table 1 The best available performance of CO_2R to CO, CH_3OH, CH_4, and syngas

	FE (%)	Current density (mA cm^{-2})	Cell voltage (V)
CO	99.7	182.2	−3.29[a]
CH_3OH	88.6	67	−3.28
CH_4	83	25.6	−1.37[b]
Syngas (H_2/CO (1:1))	47 (CO)	90.1 (CO)	−3.14[b]
Syngas (H_2/CO (2:1))	33.1 (CO)	11.4 (CO)	−2.19[b]

[a] The value was calculated on the basis of ref. 82 and experimental data; [b] The value was assumed based on ref. 96, 116 and 117.

(Fig. 1). The performance of CO_2R to CO is much better compared to targeting other C1 products (Table 1), especially, the current density for CO_2R to CO is approaching 200 mA cm^{-2}. However, for CO_2R to CH_4, the FE value is lower than 85%, and the current density is only 25.6 mA cm^{-2}, calling for more research concerns. For the syngas of H_2/CO (2:1), the current density is the lowest among the studied C1 product, which is as low as 11.4 mA cm^{-2}.

IL-based electrolytes have been developed for CO_2 to C1. Currently, the ILs with imidazolium cation are the most commonly used electrolytes and are usually beneficial to the improvement of CO_2R performance through the formation of the CO_2-imidazolium intermediate compound, which can help to reduce the overpotential of CO_2R. The viscosity, conductivity, and interaction between cations and anions of ILs can all influence the efficiency, which can be optimized by adding water or organic solvents, changing the carbon chain length of

the imidazole cation, and replacing the suitable anions. Regrettably, most studied IL-based electrolytes are concentrated on the imidazolium-based ones, and the ILs other than those of imidazolium-based as well as the effect of IL-anions have not been studied sufficiently, calling for more research. Also, the mechanism of ILs as the electrolyte in CO_2R should be deeply explored, and novel, clean, and highly efficient IL-based electrolytes with functional cations and anions need to be developed to improve the performance of CO_2R.

3. Evaluation of IL-based electrochemical CO_2 reduction to C1 products

Both, economic analysis and environmental impact depend on the performance of CO_2R and other related processes,
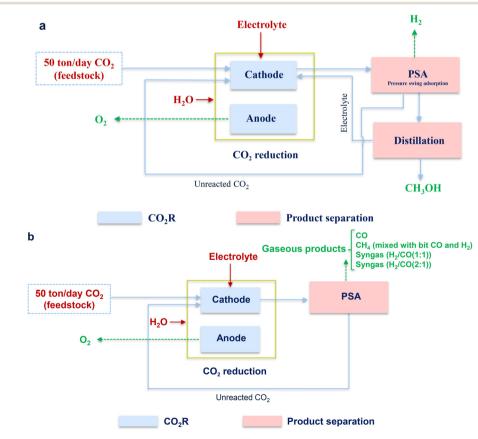

Fig. 4 The flow diagram of CO_2R to CH_3OH (a) and gaseous products (b).

© 2023 The Author(s). Co-published by the Institute of Process Engineering, Chinese Academy of Sciences and the Royal Society of Chemistry

Ind. Chem. Mater., 2023, **1**, 410–430 | **417**

such as the separation to obtain pure products. In this part, the identified parameters listed in Table 1 were used for evaluating CO_2R, and the cost estimation was based on the specific process for a different target product, and then the energy demand and environmental impact were further estimated for comparison and discussion.

3.1. Processes

As shown in Fig. 4, the whole process for all cases can be divided into two parts, namely, CO_2R and product separation, which can be liquid or gas separation, depending on the target products.

For CO_2R, a CO_2 gas stream was used as the feedstock and injected into the cathode chamber for the reduction to obtain the products. The unit of CO_2R was assumed as a black-box model since it is still at the bench scale, in which the main and parasitic reaction equations are listed in Table 2. In general, by-products can be generated. In this work, when CH_3OH was targeted, H_2 was considered to be the only by-product. On the contrary, the production of H_2 was ignored due to the extremely high CO selectivity when CO was the targeted product. For the case of CH_4 production via CO_2R, H_2, and CO were considered as the by-products, while no other by-products were considered. As for syngas comprising CO and H_2, there were no other gaseous and liquid products generated. For all the cases, oxygen evolution took place in the anode chamber.

After CO_2R, the separation unit was followed for different purposes. When the gaseous product (CO, CH_4, or syngas) was obtained as the products from CO_2R, the unreacted CO_2 was separated from the targeted product with pressure swing adsorption (PSA) and returned to the cathode compartment; while in terms of CH_3OH as the targeted product, an additional unit of distillation was used to separate the liquid product (CH_3OH) from the electrolyte. Notably, the further purification of CH_4, i.e., the removal of the small amounts of H_2 and CO was excluded as H_2 and CO could also be considered as energy gases or reducing agents. For all the cases, it was assumed that the (regenerated) electrolyte was recycled back to the electrolyzer without any waste and loss.

3.2. Scenarios of CO_2R

CO_2R is a relatively new technology, which has been investigated intensively with great and rapid progress, as

Table 2 Reactions during CO_2R

Products	Cathode	Anode
CO	$CO_2 + H^+ + 2e^- \rightarrow CO + H_2O$ $2H^+ + 2e^- \rightarrow H_2$	$2H_2O - 4e^- \rightarrow O_2 + 4H^+$
CH_3OH	$CO_2 + 6H^+ + 6e^- \rightarrow CH_3OH + H_2O$ $2H^+ + 2e^- \rightarrow H_2$	
CH_4	$CO_2 + 8H^+ + 8e^- \rightarrow CH_4 + 2H_2O$ $CO_2 + H^+ + 2e^- \rightarrow CO + H_2O$ $2H^+ + 2e^- \rightarrow H_2$	
Syngas	$CO_2 + H^+ + 2e^- \rightarrow CO + H_2O$ $2H^+ + 2e^- \rightarrow H_2$	

Table 3 The parameters used in the base and future cases

	Base case	Case 1	Case 2	Case 3
CO as the target product				
Current density (mA cm^{-2})	182.2	200	400	600
FE (%)	99.7	99.7	99.7	99.7
Cell voltage (V)	3.29	3	2.5	2
CH_3OH as the target product				
Current density (mA cm^{-2})	67	200	400	600
FE (%)	88.6	90	95	99
Cell voltage (V)	3.28	3	2.5	1.5
CH_4 as the target product				
Current density (mA cm^{-2})	25.6	200	400	600
FE (%)	83	90	95	99
Cell voltage (V)	1.37	1.3	1.25	1.2
Syngas (H_2/CO (1:1)) as the target product				
Current density (mA cm^{-2}), CO	90.1	200	400	600
FE (%), CO	47	47	47	47
Cell voltage (V)	3.14	2.5	2	1.5
Syngas (H_2/CO (2:1)) as target product				
Current density (mA cm^{-2}), CO	11.4	200	400	600
FE (%), CO	33.1	33.1	33.1	33.1
Cell voltage (V)	2.19	2	1.5	1.34

summarized in section 2. It is expected that more progress will be achieved in the coming years. To evaluate the process fairly, in this work, both the current status and future potential cases were considered, i.e., one base case using the identified parameters listed in Table 1, which are also summarized in Table 3, and three future cases with further development of CO_2R, e.g., cell voltage, current density, and FE (shown in Table 3), which was based on the development in recent two years as well as the performance of CO_2R with other electrolytes.[119,120] The other used parameters and assumptions are listed in Table S1.†

3.3. Economic analysis

The total production cost (TPC) was the summation of the annual capital cost (ACC) and the total operating cost (TOC),[121] which was used as the criterion to evaluate the economic benefit of CO_2R by comparing it with the current market price for each case.

3.3.1 Annual capital cost. ACC was related to the total capital cost (TCC), interest rate (i), and project lifetime (L). In this work, ACC was estimated according to eqn (1).[58] The components for calculating TCC are listed in Table 4.

$$ACC = \frac{TCC}{\left(1 - (1+i)^{-L}\right)/i} \tag{1}$$

3.3.2 Total capital cost. The total capital cost briefly includes two parts: the CO_2R electrolyzer and other auxiliary equipment.[58] For the CO_2R electrolyzer, no industrial scale has been implemented, making it difficult to determine its capital cost directly. Since CO_2R is similar to water electrolysis, the main components of the water electrolysis electrolyzer were used as the reference for those in the CO_2R electrolyzer. Currently, there are two types of electrolyzers for commercial water electrolysis, i.e., alkaline and proton

Table 4 The components of TCC and TOC

Total capital cost (TCC)		Total operating cost (TOC)	
Direct cost (DC)[60]	Percentage of DC (%)	Variable operating cost value (VOC)[58]	
Electrolyzer cost	65	CO_2 feed cost	The amount of CO_2 consumed × price
BoP cost	35	IL make-up	The amount of IL make-up × price
Indirect cost (IC)[122]	Percentage of DC (%)	Organic solvent make-up	The amount of organic solvent make-up × price
Contingency	15	H_2O cost	The amount of H_2O consumed × price
Site preparation	2	Electricity cost	The power demand × electricity price
Engineering and design	8		
Up-front permitting	15		
	Percentage of FCC[a] (%)	Fixed operating cost (FOC)	Percentage of DC (%)
Working capital	5	Operation and maintenance	3.2
PSA	Calculated based on Table S2†		
Distillation	Calculated based on Table S3†	PSA[123]	Calculated based on Table S2†
Initial solvent cost	Initial input quantity × price	Distillation[124]	Calculated based on Table S3†
Initial catalyst cost	Initial input quantity × price		
TCC	Sum of the above costs	TOC	Sum of the above costs

exchange membrane (PEM) electrolysis, where the current densities are usually <1 and 1–2 A cm^{-2}, respectively.[125,126] Given that the highest current density is below 1 A cm^{-2}, similar to the previous work,[58] in this work, the capital cost of the CO_2R electrolyzer was calculated according to the H2A model for an alkaline water electrolyzer from the US Department of Energy (DOE).[60,127] The total required electrolyzer area (TEA), as an important parameter, can be calculated using the following eqn (2) and (3).[58]

$$I = \frac{m_p \times z_p \times F}{M_p \times FE_p} \quad (2)$$

$$TEA = \frac{I}{j} \quad (3)$$

where m_p and M_p are the production rate and molar mass of the product, respectively, FE_p and z_p are the faradic efficiency (FE) and demanded electrons number, respectively, for each product, F is the faradic's constant (96 485 C mol^{-1}), and I and j are the total current and current density through the electrolysis, respectively.

The equipment costs for PSA and distillation were calculated on the basis of ref. 123 and 124 according to eqn (4).[128]

$$C = C_{ref} \times \left(\frac{S}{S_{ref}}\right)^n \quad (4)$$

where C and S are the investment cost and the scaling size of the PSA/distillation unit, respectively, while C_{ref} and S_{ref} correspond to the data from references, and n is the scale factor. The chemical engineering plant cost index (CEPCI) was used to extrapolate the cost estimations to the price level of 2022.

The expenditure of the initial electrolyte and cathode catalyst was considered in the capital cost, which was independently calculated by multiplying the univalence of the item and its mass consumption. The main parameters and the counting process are described in the ESI.†

3.3.3 Total operating cost. The total operating cost (TOC) consists of variable and fixed operating costs. The components for calculating TOC are listed in Table 4. Here, we considered

that the cost for operation and maintenance, as the only fixed operating cost, was 3.2% of the direct cost (DC). The variable operating cost was from materials, such as the CO_2 feed, electrolyte, H_2O, and electricity. Our preliminary study showed that the electricity price was a major contributor, which was calculated based on the basis of the demanded power (P) and electricity price in this work. The demanded power can be obtained by the following eqn (5).[58]

$$P = V \times I = V \times \frac{m_p \times z_p \times F}{M_p \times FE_p} \quad (5)$$

where V is the cell voltage.

Additionally, the operating costs for PAS and distillation were calculated independently, as shown in the ESI.†

3.3.4 Results and discussion on economic analysis. The values of TPC of CO, CH_3OH, CH_4, and syngas were calculated under the condition of the base case. The estimation results are shown in Fig. 5a, where the market price for each product is also illustrated as a "box", i.e., in a range, according to the literature survey combined with the further explanation as follows.[58,60,129–133] For the syngas, both its TPC and the market price were assessed via those of CO in the syngas, and the upper limit value represents the syngas from the basic oxygen furnace gas (BOFG) and the low limit value was for the syngas from corn stover.[129]

Among all the studied products, CO was found to be the only profitable product for CO_2R with ILs as electrolytes at the present status. While for other products, their TPCs were still too high to be profitable, and especially for CH_4 and H_2/CO (2 : 1), their TPCs were 4.09 and 2.99 € per kg, respectively, far away from the market prices (0.18–0.35 and 0.03–0.54 € per kg, respectively). This observation was, on the one hand, in line with the achievement of CO_2R, where the current density and FE for CO were already up to 182.2 mA cm^{-2} and 99.7%, respectively, while for CH_4 and H_2/CO (2 : 1), their current densities were as low as 25.6 and 11.4 mA cm^{-2}, respectively, together with low FE (Table 1). On the other hand, the relatively low market price of CH_4 and H_2/CO (2 : 1)
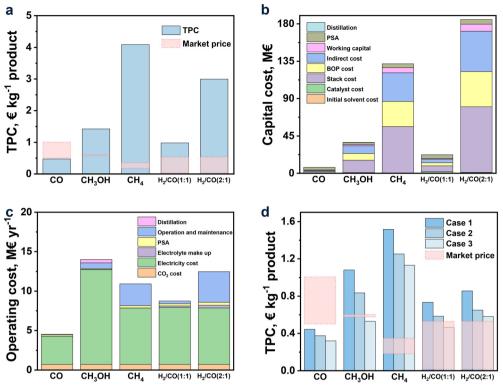
© 2023 The Author(s). Co-published by the Institute of Process Engineering, Chinese Academy of Sciences and the Royal Society of Chemistry

Ind. Chem. Mater., 2023, **1**, 410–430 | **419**

Fig. 5 (a) TPC; (b) capital cost and (c) operating cost for CO_2R to CO, CH_3OH, CH_4, and syngas (H_2/CO (1:1) and H_2/CO (2:1)) in the base case; (d) TPC for each product in the future cases.

can be another reason, which was further discussed later in this work.

To further analyze, the detailed capital cost is shown in Fig. 5b. As we can see, the TCC of CO was quite low, followed by H_2/CO (1:1) and CH_3OH, while those of CH_4 and H_2/CO (1:2) were much higher. Compared to CO, the BoP and stack costs for CH_3OH, CH_4, H_2/CO (1:1) and H_2/CO (2:1) were much higher, owing to the lower current density and thus higher electrolyzer area. The high costs of BoP and stack lead to high indirect costs. The summations of (indirect, BoP, and stack costs) for H_2/CO (1:1), CH_3OH, CH_4, and H_2/CO (2:1) contribute to 67.6, 87.0, 91.7, and 91.8% in TCC, respectively, and this trend is opposite to that of their current densities in CO_2R, further indicating the vital role of the current density on TCC. As the current densities for products other than CO are still low, it is important to further develop CO_2R to improve the performance and then make it possible to achieve desirable results in the near future.

According to the detailed operating cost shown in Fig. 5c, the most intensive part was the electricity usage, which was closely linked to the cell voltage and FE. The yearly (operation and maintenance) cost was also the main expenditure for CH_4 and H_2/CO (1:1) due to the high investment cost reflected by the direct capital cost. As to CH_3OH, the capital cost for the distillation was also the obvious part due to the low concentration of CH_3OH (30 wt%) in the electrolyte that requires high energy demand for its separation.[134]

As discussed above, the performance of CO_2R, including current density, cell voltage, and FE, had a great influence on

TPC. This implied that the development status of CO_2R was of importance in cost estimation. According to section 2, the development of CO_2R was vital all these years, and performance improvement was rapid, making it essential to predict the cost based on the results that can be achieved in the near future. Hence, in this part, three future cases for each product, along with the improvement of current density and FE as well as the diminishing of cell voltage were assumed, according to the research results in recent years and those for the CO_2R using electrolytes other than ILs.[119,120] The results are shown in Fig. 5d.

Overall, TPCs evidently declined with the hypothetical augmented performance of CO_2R. For CO, TPC was decreased to 0.32 € per kg, approaching half of the low limit market price (0.5 € per kg) when the current density was enhanced to 600 mA cm^{-2} and the cell voltage descended to 2 V, manifesting the perspective to set CO as the target product in CO_2R. As for CH_3OH, it can be profitable when the current density and FE reach 600 mA cm^{-2} and 99%, respectively, and the cell voltage drops to 1.5 V. For the syngas of H_2/CO (1:1), under the situation of case 3, its TPC would be lower to the price for that from the corn stover (0.54 € per kg). However, for CH_4 and H_2/CO (2:1), their TPCs were still much higher than the market price even though with a dramatic improvement in their performance of CO_2R within the created scenarios.

To find out how the CH_4 and syngas (H_2/CO (2:1)) could be profitable, the current density of 1000 mA cm^{-2} (the industrial performance of PEM for commercial water

electrolysis),[125,135] FE of 100%, and the cell voltage of 1.06 V for CH$_4$ and 1.34 V for syngas (the standard cell voltage)[136] were assumed, and the corresponding TPCs were estimated. As a result, the TPC of H$_2$/CO (2:1) just reached the upper limit market price, but still, it remains unprofitable for CH$_4$. This observation suggested that CH$_4$ as the target product was an undesirable path of CO$_2$R. There may be two reasons for the unprofitable of CO$_2$R to CH$_4$. One is the low market price, and the other is the highest electron demand (8e$^-$) for the formation of CH$_4$ among the different paths of CO$_2$R to C1 products.[9,38,89,95,96]

3.3.5 Sensitivity analysis and discussion. To obtain a comprehensive insight into how the key parameters affect the TPCs of C1 products generated from CO$_2$R, sensitivity analyses were conducted under two assumed scenarios (better and worse cases) based on the base case. The parameters, including current density, FE, cell voltage, CO$_2$ price, electricity price, and stack price, were considered. Compared to the base case, all the parameters varied up and down by 20% in the better and worse cases, respectively. In the calculation, one parameter changed while the other parameters remained consistent with the base case. It should be pointed out that FE was set as 100% in the better case when CO and CH$_3$OH were the target products because there was only a small space for further improvement. For syngases of H$_2$/CO (1:1) and H$_2$/CO (2:1) as the target products, FE was not considered due to the fixed ratio.

In Fig. 6, the results of TPC for each product under the base, better and worse cases are exhibited via orange, green,

and purple bars, respectively. Overall, FE was the most influential factor, while the effect of CO$_2$ price can be negligible for all the products. The effect degrees of current density and cell voltage on the TPC of each product depended on the performance of CO$_2$R itself. For example, when the current density improved by 20%, the TPCs of CO (the current density of 182.2 mA cm^{-2} in the base case) and syngas of H$_2$/CO (2:1) (the current density of 11.4 mA cm^{-2} in the base case) decreased by 1.6 and 12.3%, respectively. Similarly, when the cell voltage decreased by 20%, the TPCs of CO (the cell voltage of 3.29 V in the base case) and syngas of H$_2$/CO (2:1) (the cell voltage of 2.19 V in the base case) decreased by 13.3 and 4.2%, respectively. These results suggest that the slight change in the current density and cell voltage can lead to an obvious variation in TPCs when the performance of CO$_2$R itself is relatively poor. Additionally, the 20% fluctuation in electricity and stack prices can cause an obvious change in TPC, as shown in Fig. 6 for all the studied products.

3.4. Environment assessment

The life cycle assessment (LCA) was used to assess the environmental impacts of "CO$_2$R to product" based on the ISO 14040/14044 framework, and the global warming impact (GWI) was selected as the main indicator.[134] Herein, the total amount of CO$_2$ emitted from the CO$_2$R process was evaluated via the cradle-to-gate LCA method to account for all sources of CO$_2$ emissions in each unit. Finally, the amounts of CO$_2$
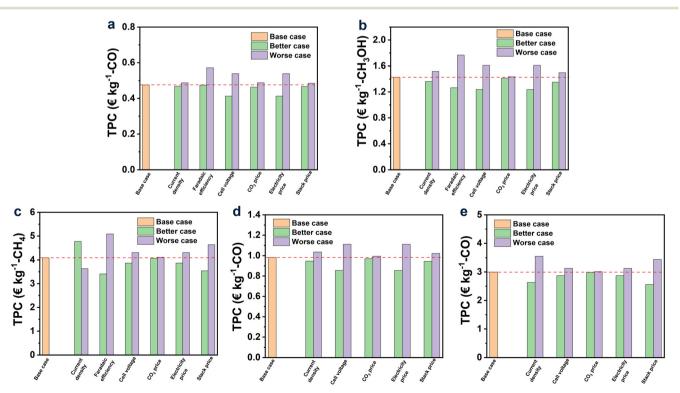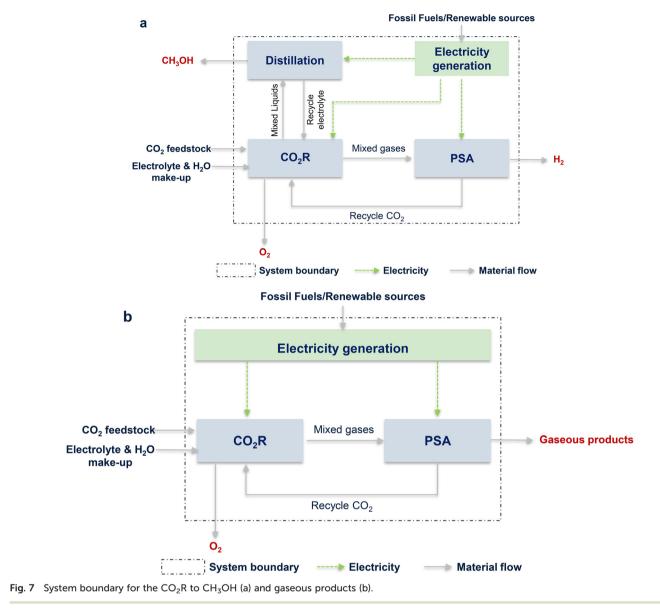

Fig. 6 Sensitivity analysis for CO$_2$R to C1 products under better and worse cases with different parameters, (a) CO; (b) CH$_3$OH; (c) CH$_4$; (d) syngas of H$_2$/CO (1:1) and (e) syngas of H$_2$/CO (2:1).

© 2023 The Author(s). Co-published by the Institute of Process Engineering, Chinese Academy of Sciences and the Royal Society of Chemistry

Ind. Chem. Mater., 2023, **1**, 410–430 | **421**

a

Fossil Fuels/Renewable sources

CH_3OH ← **Distillation** ⇠ **Electricity generation**

Mixed Liquids | Recycle electrolyte

CO_2 feedstock → | **CO_2R** | Mixed gases → | **PSA** | → H_2
Electrolyte & H_2O make-up →

Recycle CO_2

O_2

┄┈ System boundary ⇢ Electricity → Material flow

b

Fossil Fuels/Renewable sources

Electricity generation

CO_2 feedstock → | **CO_2R** | Mixed gases → | **PSA** | → Gaseous products
Electrolyte & H_2O make-up →

Recycle CO_2

O_2

┄┈ System boundary ⇢ Electricity → Material flow

Fig. 7 System boundary for the CO_2R to CH_3OH (a) and gaseous products (b).

emissions were obtained for the assessment. It should be noted that the environmental burdens of by-products (such as H_2 and O_2) were also considered. The system boundary is shown in Fig. 7. GWI was calculated based on the electricity

generation intensity and electrical energy required in each unit. The calculation process is described in the ESI.†

As described in the above paragraph, the calculation of GWI was based on electricity, *i.e.*, LCA strongly depends on
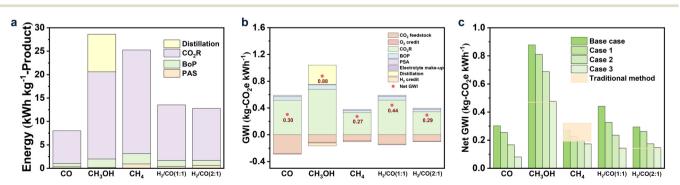
Fig. 8 The demanded energy (a) and GWI breakdown (b) for each product under the base case; as well as net GWI (c) for each product under the base and future cases.

energy usage.[137–139] Here the energy demands, including CO_2R, BoP, and PSA units and the additional distillation unit for CH_3OH, for producing one kg of CO, CH_3OH, CH_4, and syngas were calculated. The results are depicted in Fig. 8a. Obviously, the electricity usage of the CO_2R unit was the major part for all the products, accounting for more than 80% when CO, CH_4, or syngas was the product and more than 50% for CH_3OH as the target product. Different from other products, the production of CH_3OH requires separating the liquid product CH_3OH from the electrolyte, and the corresponding energy demand was another main contributor. Comparatively, the energy usages for BoP and gas separation were insignificant for all the products.

Overall, the energy demand for producing one kg-CH_3OH was higher than that of CO or syngas, which was ascribed to the additional energy usage from the distillation unit due to its low concentration (30 wt%).[134] For CH_4, the total energy usage was also higher than that for CO and syngas, and the corresponding energy demand of the CO_2R unit was higher than that for CH_3OH, which was attributed to its suboptimal performance, such as low current density, unsatisfactory FE, and high cell voltage.

The CO_2 emissions per kW h, containing the CO_2 footprint of all the co-product credits, energy usage, and raw materials, were calculated to appraise their GWI, thereby, their environmental impact, owing to its tight relationship with the global warming potential. Noteworthily, in this evaluation process, the GWI of CO_2 feedstock was calculated based on the carbon footprint of −0.5 kg-CO_2e per kg-captured-CO_2 taken from the literature.[140] Fig. 8b shows the GWI breakdown for the five products in CO_2 feedstock, CO_2R, and separation under the base case, where the solid circle represents the net GWI. As indicated in Fig. 8b, the GWI for producing CH_3OH was the highest (0.88 kg-CO_2e per kW h) among the studied products, which was also higher than that of the coal-to-CH_3OH process (0.47 kg-CO_2e per kW h) due to the intensive energy usages for CO_2R and liquid-separation. The GWI of CH_4 was the lowest (0.27 kg-CO_2e per kW h) among the five products, which was also comparable to that of the thermochemical CO_2 conversion (0.19–0.32 kg-CO_2e per kW h).[134,141] This result suggested that CH_4 was the most suitable product from the environment-friendly aspect. For the syngas of H_2/CO (2 : 1), the GWI (0.29 kg-CO_2e per kW h) of the CO_2R route was higher than that of the traditional method (0.14 kg-CO_2e per kW h).[142] As for CO and H_2/CO (1 : 1), to the best of our knowledge, no GWI value has been reported. Since the GWI of CO (0.30 kg-CO_2e per kW h) was similar to that of CH_4 and syngas of H_2/CO (2 : 1), CO was a more attractive product than CH_3OH and H_2/CO (1 : 1), indicating that the path of CO_2R to CO was also beneficial for the environment.

For the future cases, with the hypothetically improved CO_2R performance, the net GWI was distinctly decreased, as shown in Fig. 8c. For example, for CH_4, when the FE and current density were increased to 99% and 600 mA cm^{-2}, respectively, as well as the cell voltage was decreased to 1.2 V, the net GEI of

CH_4 was sharply declined from 0.27 to 0.17 kg-CO_2e per kW h, which was lower than that of thermochemical CO_2 conversion (0.19 kg-CO_2e per kW h). When CH_3OH and H_2/CO (2 : 1) were set as the target products, under the most desirable case (case 3), the net GWI of CO_2R was almost comparable to the traditional method. The net GWIs of the CO_2R to CO and H_2/CO (1 : 1) were also greatly decreased from 0.3 and 0.44 kg-CO_2e per kW h to 0.08 and 0.14 kg-CO_2e per kW h, respectively. Therefore, CO_2R is a promising path to reaching environment-friendly requirements.

Combining the environmental assessment with the economic analysis, CO_2R to CO is a desirable pathway for CO_2R, even in the current situation. In the future, with the further improvement of CO_2R, CH_3OH and H_2/CO (1 : 1) will be desirable routes. However, for CH_4 and H_2/CO (2 : 1), the unfavorable economic results of CO_2R make it challenging to compete with other routes. Adding H_2 produced from other routes to H_2/CO (1 : 1) and thus forming H_2/CO (2 : 1) can be an alternative way, which will be studied in our future work.

This work summarized and evaluated the CO_2R using IL-based electrolytes. There has been much research work conducted on other systems using electrolytes other than IL-based, and the performance can be better than that with ILs listed in this work. For example, for CO, the current density was over 300 mA cm^{-2}.[119,120] Such results further indicate the prospectives of CO_2R and the reasonability of the assumed parameters for the future case. We expect that the development of CO_2R, together with ILs, will greatly improve the performance in the foreseen future.

It should also be pointed out that for future cases (cases 1 to 3), in this work, only the parameters linked to the CO_2R performance were adjusted, while in principle, other parameters, such as CO_2 price, electricity, and product price also need to be considered. However, based on the sensitivity analysis, the CO_2 price has a limited influence on the TPC for all studied products. Given the unstable variation tendency of electricity prices last year and other uncertainties linked to war and politics, it is difficult to make reasonable assumptions about electricity prices in the future. Similarly, reasonably assuming future product prices is another puzzle, which involves a deep knowledge of different industrial technologies. Therefore, it is reasonable to fix the parameters as the base case for the parameters of CO_2 price, electricity, and product price in future cases.

Additionally, industrialization is mandatory for CO_2R to achieve commercial value. The current density and product selectivity are required to be over 200 mA cm^{-2} and 90%, respectively, for industrial applications. This is in line with the results obtained from the section on economic analysis. Therefore, except for CO, the performance of CO_2R to other products needs to be greatly improved. Besides, research on the stability of CO_2R systems at the industrial level should be performed in future studies.[143] Meanwhile, from the sensitivity analysis, the enhancement of CO_2R performance, including current density, FE, and cell voltage, are the keys to reducing TPC, especially for CH_3OH and syngas of H_2/CO (1 :

© 2023 The Author(s). Co-published by the Institute of Process Engineering, Chinese Academy of Sciences and the Royal Society of Chemistry

Ind. Chem. Mater., 2023, **1**, 410–430 | **423**

1). While it is difficult for CH_4 and syngas H_2/CO (2:1) to be profitable *via* only improving the performance of CO_2R due to the low energy efficiency. Developing a novel electrolyzer might be a choice for CH_4 to be profitable. As to syngas H_2/CO (2:1), integrating CO_2R with commercial hydrogen production may maximize its economic benefits.

4. Comparison of traditional and ionic liquids–based electrolytes

The electrolyte is a vital consideration apart from the extensively studied electrocatalysts to achieve the satisfactory performance of CO_2R *via* controlling reduction surrounding at the interface between electrocatalyst and electrolyte, dissolving the reactant CO_2, and stabilizing the reaction intermediates.[10] Traditional electrolytes, including the aqueous of sodium or potassium salts and organic solvents (*e.g.*, MeCN, DMF, DMSO, and acetone), have been widely used in CO_2R. Potassium or sodium solutions have good electrical conductivity while a fairly limited ability to dissolve CO_2 (<34 mM under the standard condition).[144] Besides, the undesirable HER side reaction is easier to occur in these aqueous solutions. Normally, the solubility of CO_2 in the organic solvent is higher than that in the aqueous electrolyte solutions. For example, the solubility of CO_2 in MeCN (270 mM) is approximately 9 times as high as that in aqueous electrolyte solutions.[145] However, the current density of CO_2R with organic solvents is low, although they can effectively inhibit HER, which limits their further large-scale application.[146] IL-based electrolytes with high CO_2 solubility, as discussed above, not only have unique properties in promoting the performance of CO_2R but also can be the activator of CO_2 and stabilizer of $CO_2^{\cdot-}$, which have been increasingly studied and developed in these years, as summarized in this work and other review articles.[13,26,42,46,67] Nevertheless, when IL-based electrolytes are used to replace traditional electrolytes, the economic (cost, stability) and environmental influence are usually questioned. Therefore, traditional and IL-based electrolytes were further analyzed and compared from economic and environmental aspects.

The market price of traditional electrolytes is indeed lower than that of ILs, which is about 3400, 2876, and 205 € per ton to MeCN,[147] DMF,[148] and $NaCO_3$,[149] respectively, while it is 5800 € per ton to ILs.[58] However, when CO is set as the target product of CO_2R, the proportions of IL cost are as low as 0.3 and 0.02% in TCC and TOC, respectively. This situation is similar to the other products, suggesting that the market price of ILs will not hamper the use of ILs as electrolytes in CO_2R. Additionally, the long-term stability of electrolytes is beneficial for cost saving. For industrialization, the stability of the CO_2R system should reach at least 80 000 h.[143] Regrettably, there is no study on the stability of electrolytes at the industrial level. While CO_2R with IL-based electrolytes shows comparable stability to that with traditional electrolytes in a large number of studies. Moreover, Yuan *et al.*[150] found that the CO selectivity in the

IL-based electrolytes is 51.3% higher than that in 0.1 M $KHCO_3$ aqueous electrolytes after 10 h of continuous operation in an upscaling modified H-type cell, suggesting the higher stability of IL-based electrolytes. Therefore, IL-based electrolyte is not inferior to traditional electrolytes from the economic aspects.

As to the environment, ILs are considered "green solvents" because of their negligible volatility and flammability as well as high stability. However, the statement on "green solvents" for ILs has been questioned in recent years, because it lacks a comprehensive understanding of their toxicity and biodegradability. Given this, Costa and co-workers[151] summarized and updated the relevant data on the toxicity and (bio)degradability of ILs. This work showed that the commonly used ILs with *N*-substitution cations or fluoride anions were resistant to biodegradation, which, however, can be improved through functionalizing the imidazole cations. Bystrzanowska *et al.*[152] evaluated the greenness of more than 300 commercially available ILs and ranked them with organic solvents from the toxicity to organisms, biodegradability, hazard statements, and precautionary measures when handling them. As a result, the most commonly used ILs, including 1-ethyl-3-methylimidazolium bis(trifluoromethylsulfonyl)imide ([Emim][Tf$_2$N]), [Bmim][BF$_4$], and [Bmim]Br, were ranked between polar and nonpolar molecular solvents in terms of greenness. Comprehensively, ILs appear to be more resistant to biodegradation and toxicity than traditional electrolytes. Nevertheless, traditional electrolytes, such as DMF and MeCN, can cause direct harm to human beings through touch and breath.[153] On the contrary, ILs have little impact on researchers, especially under normal pressure and temperature as those operated within CO_2R. Moreover, ILs as the electrolyte in CO_2R are usually used in small quantities and can be recycled. Therefore, devoting more efforts to designing and synthesizing novel effective ILs with low toxicity and high biodegradability as electrolytes are necessary as they will be meaningful for the future development of CO_2R considering the unique superiority of ILs in promoting the performance of CO_2R.

5. Conclusions

An instant literature survey on the CO_2R to C1 products (CO, CH_3OH, CH_4, and syngas) with ILs-based electrolytes was conducted summarizing the most recent results from the past two years, and the best performance for each target product was identified. The literature survey shows that CO_2R to CO was mostly studied in the recent two years, and desirable performance has been achieved (FE of 99.7% and current density of 182.2 mA cm^{-2}); for CO_2R to other studied C1 products, much fewer studies were conducted, and the performance needs to be further improved.

The economic analysis and environmental assessment of CO_2R to C1-product were estimated, where both the parameters of the state-of-the-art (base case) and future cases with improved performance (cases 1 to 3) were used. Currently, CO is the only profitable product, in the future,

CH_3OH and the syngas of H_2/CO (1:1) will achieve profitability, but CH_4 and the syngas of H_2/CO (2:1) will always be unprofitable. For the environmental impact, CH_4 is the most environmentally friendly product from CO_2R, followed by the syngas of H_2/CO (2:1) and CO, and then CH_3OH, and the desirable CO_2R performance will make CO_2R to C1-products an environmentally friendly pathway. Overall, CO_2R-to-CO is the most profitable path considering both economic and environmental aspects.

Summarily, for CO_2R with IL-based electrolytes, the pathway of CO_2R to CO has shown commercial potential based on the state-of-the-art achievement at the laboratory level from both economic and environmental aspects. For the other products, more efforts are needed to be implemented to improve the CO_2R performance or develop more advanced electrolyzers (e.g., GDE-type electrolyzer, membrane electrode assembly-type electrolyzer, microfluidic-type electrolyzer, and solid-state electrolyte-type electrolyzer). Furthermore, ILs should be further exploited in future CO_2R as follows: (1) the adjustable feature of ILs in the structure and properties provides unique advantages and feasibilities for designing more efficient and suitable electrolytes of CO_2R; (2) the capability of ILs to dissolve a variety of solvents and electrolytes can integrate other solvents and electrolytes, further improving the performance of CO_2R; (3) the cleaner ILs can be designed and synthesized applying into CO_2R to mitigate the environmental burden; (4) except as electrolytes, ILs can also be the co-catalyst or modifier for the catalyst exhibiting prominent performance.

Conflicts of interest

The authors declare no conflict of interest.

Acknowledgements

References

1 J. Lelieveld, K. Klingmuller, A. Pozzer, R. T. Burnett, A. Haines and V. Ramanathan, Effects of fossil fuel and total anthropogenic emission removal on public health and climate, *Proc. Natl. Acad. Sci. U. S. A.*, 2019, **116**, 7192–7197.

2 M. M. F. Hasan, L. M. Rossi, D. P. Debecker, K. C. Leonard, Z. Li, B. C. E. Makhubela, C. Zhao and A. Kleij, Can CO_2 and renewable carbon be primary resources for sustainable fuels and chemicals?, *ACS Sustainable Chem. Eng.*, 2021, **9**, 12427–12430.

3 M. Takht Ravanchi and S. Sahebdelfar, Catalytic conversions of CO_2 to help mitigate climate change: Recent process developments, *Process Saf. Environ. Prot.*, 2021, **145**, 172–194.

4 L. Desport and S. Selosse, An overview of CO_2 capture and utilization in energy models, *Resour., Conserv. Recycl.*, 2022, **180**, 106150.

5 Z. Li, T. Yang, S. Yuan, Y. Yin, E. J. Devid, Q. Huang, D. Auerbach and A. W. Kleyn, Boudouard reaction driven by thermal plasma for efficient CO_2 conversion and energy storage, *J. Energy Chem.*, 2020, **45**, 128–134.

6 S. R. Sun, H. X. Wang, D. H. Mei, X. Tu and A. Bogaerts, CO_2 conversion in a gliding arc plasma: Performance improvement based on chemical reaction modeling, *J. CO2 Util.*, 2017, **17**, 220–234.

7 S. Cantera, D. Tamarit, P. J. Strong, I. Sánchez-Andrea, T. J. G. Ettema and D. Z. Sousa, Prospective CO_2 and CO bioconversion into ectoines using novel microbial platforms, *Rev. Environ. Sci. Bio/Technol.*, 2022, **21**, 571–581.

8 D. D. Ma, S. G. Han, C. Cao, X. Li, X. T. Wu and Q. L. Zhu, Remarkable electrocatalytic CO_2 reduction with ultrahigh CO/H_2 ratio over single-molecularly immobilized pyrrolidinonyl nickel phthalocyanine, *Appl. Catal., B*, 2020, **264**, 118530.

9 T. Zhang, W. Li, K. Huang, H. Guo, Z. Li, Y. Fang, R. M. Yadav, V. Shanov, P. M. Ajayan, L. Wang, C. Lian and J. Wu, Regulation of functional groups on graphene quantum dots directs selective CO_2 to CH_4 conversion, *Nat. Commun.*, 2021, **12**, 5265.

10 M. Mourade Salles Pupo and R. Kortlever, Electrolyte effects on the electrochemical reduction of CO_2, *ChemPhysChem*, 2019, **20**, 2926–2935.

11 G. Tang, J. Li, Y. Lu, T. Song, S. Yin, G. Mao, B. Long, A. Ali and G. J. Deng, Donor-acceptor organic polymer with sulfur bridge for superior photocatalytic CO_2 reduction to CH_4 under visible light illumination, *Chem. Eng. J.*, 2023, **451**, 138744.

12 A. Pan, X. Ma, S. Huang, Y. Wu, M. Jia, Y. Shi, Y. Liu, P. H. Wangyang, L. He and Y. Liu, $CsPbBr_3$ perovskite nanocrystal grown on mxene nanosheets for enhanced photoelectric detection and photocatalytic CO_2 reduction, *J. Phys. Chem. Lett.*, 2019, **10**, 6590–6597.

13 Q. Lu and F. Jiao, Electrochemical CO_2 reduction: Electrocatalyst, reaction mechanism, and process engineering, *Nano Energy*, 2016, **29**, 439–456.

14 B. V. Mathiesen, H. Lund and K. Karlsson, 100% renewable energy systems, climate mitigation and economic growth, *Appl. Energy*, 2011, **88**, 488–501.

15 N. L. Panwar, S. C. Kaushik and S. Kothari, Role of renewable energy sources in environmental protection: A review, *Renewable Sustainable Energy Rev.*, 2011, **15**, 1513–1524.

16 W. Lai, Y. Qiao, J. Zhang, Z. Lin and H. Huang, Design strategies for markedly enhancing energy efficiency in the electrocatalytic CO_2 reduction reaction, *Energy Environ. Sci.*, 2022, **15**, 3603–3629.

© 2023 The Author(s). Co-published by the Institute of Process Engineering, Chinese Academy of Sciences and the Royal Society of Chemistry

Ind. Chem. Mater., 2023, **1**, 410–430 | **425**

17 H. Kim, H. S. Jeon, M. S. Jee, E. B. Nursanto, J. P. Singh, K. Chae, Y. J. Hwang and B. K. Min, Contributors to enhanced CO_2 electroreduction activity and stability in a nanostructured Au electrocatalyst, *ChemSusChem*, 2016, **9**, 2097–2102.

18 S. Zhao, Z. Tang, S. Guo, M. Han, C. Zhu, Y. Zhou, L. Bai, J. Gao, H. Huang, Y. Li, Y. Liu and Z. Kang, Enhanced activity for CO_2 electroreduction on a highly active and stable ternary Au-CDots-C_3N_4 electrocatalyst, *ACS Catal.*, 2017, **8**, 188–197.

19 Y. S. Ham, S. Choe, M. J. Kim, T. Lim, S. K. Kim and J. J. Kim, Electrodeposited Ag catalysts for the electrochemical reduction of CO_2 to CO, *Appl. Catal., B*, 2017, **208**, 35–43.

20 C. Kim, T. Eom, M. S. Jee, H. Jung, H. Kim, B. K. Min and Y. J. Hwang, Insight into electrochemical CO_2 reduction on surface-molecule-mediated Ag nanoparticles, *ACS Catal.*, 2016, **7**, 779–785.

21 C. Jiménez, J. García, R. Camarillo, F. Martínez and J. Rincón, Electrochemical CO_2 reduction to fuels using Pt/CNT catalysts synthesized in supercritical medium, *Energy Fuels*, 2017, **31**, 3038–3046.

22 M. Ma, H. A. Hansen, M. Valenti, Z. Wang, A. Cao, M. Dong and W. A. Smith, Electrochemical reduction of CO_2 on compositionally variant Au-Pt bimetallic thin films, *Nano Energy*, 2017, **42**, 51–57.

23 T. Ilyas, F. Raziq, S. Ali, A. Zada, N. Ilyas, R. Shaha, Y. Wang and L. Qiao, Facile synthesis of MoS_2/Cu as trifunctional catalyst for electrochemical overall water splitting and photocatalytic CO_2 conversion, *Mater. Des.*, 2021, **204**, 109674.

24 N. Hussain, M. A. Abdelkareem, H. Alawadhi, A. H. Alami and K. Elsaid, Cu_2O nanoparticles decorated with MoS_2 sheets for electrochemical reduction of CO_2 with enhanced efficiency, *Appl. Phys. A: Mater. Sci. Process.*, 2022, **128**, 131.

25 J. Ye, D. Rao and X. Yan, Regulating the electronic properties of $MoSe_2$ to improve its CO_2 electrocatalytic reduction performance via atomic doping, *New J. Chem.*, 2021, **45**, 5350–5356.

26 C. Hiragond, H. Kim, J. Lee, S. Sorcar, C. Erkey and S. I. In, Electrochemical CO_2 reduction to CO catalyzed by 2D nanostructures, *Catalysts*, 2020, **10**, 98.

27 X. Yang, J. Cheng, X. Yang, Y. Xu, W. Sun and J. Zhou, MOF-derived Cu@Cu_2O heterogeneous electrocatalyst with moderate intermediates adsorption for highly selective reduction of CO_2 to methanol, *Chem. Eng. J.*, 2022, **431**, 134171.

28 P. Han, X. Yu, D. Yuan, M. Kuang, Y. Wang, A. M. Al-Enizi and G. Zheng, Defective graphene for electrocatalytic CO_2 reduction, *J. Colloid Interface Sci.*, 2019, **534**, 332–337.

29 R. A. Geioushy, M. M. Khaled, K. Alhooshani, A. S. Hakeem and A. Rinaldi, Graphene/ZnO/Cu_2O electrocatalyst for selective conversion of CO_2 into n-propanol, *Electrochim. Acta*, 2017, **245**, 456–462.

30 C. Zhang, S. Yang, J. Wu, M. Liu, S. Yazdi, M. Ren, J. Sha, J. Zhong, K. Nie, A. S. Jalilov, Z. Li, H. Li, B. I. Yakobson, Q. Wu, E. Ringe, H. Xu, P. M. Ajayan and J. M. Tour, Electrochemical CO_2 reduction with atomic iron-dispersed on nitrogen-doped graphene, *Adv. Energy Mater.*, 2018, **8**, 1703487.

31 M. Li, H. Wang, W. Luo, P. C. Sherrell, J. Chen and J. Yang, Heterogeneous single-atom catalysts for electrochemical CO_2 reduction reaction, *Adv. Mater.*, 2020, **32**, e2001848.

32 D. Grammatico, A. J. Bagnall, L. Riccardi, M. Fontecave, B. L. Su and L. Billon, Heterogenised molecular catalysts for sustainable electrochemical CO_2 reduction, *Angew. Chem., Int. Ed.*, 2022, **61**, e202206399.

33 L. Zhang, X. X. Li, Z. L. Lang, Y. Liu, J. Liu, L. Yuan, W. Y. Lu, Y. S. Xia, L. Z. Dong, D. Q. Yuan and Y. Q. Lan, Enhanced cuprophilic interactions in crystalline catalysts facilitate the highly selective electroreduction of CO_2 to CH_4, *J. Am. Chem. Soc.*, 2021, **143**, 3808–3816.

34 A. Gawel, T. Jaster, D. Siegmund, J. Holzmann, H. Lohmann, E. Klemm and U. P. Apfel, Electrochemical CO2 reduction - the macroscopic world of electrode design, reactor concepts & economic aspects, *iScience*, 2022, **25**, 104011.

35 S. Nitopi, E. Bertheussen, S. B. Scott, X. Liu, A. K. Engstfeld, S. Horch, B. Seger, I. E. L. Stephens, K. Chan, C. Hahn, J. K. Norskov, T. F. Jaramillo and I. Chorkendorff, Progress and perspectives of electrochemical CO_2 reduction on copper in aqueous electrolyte, *Chem. Rev.*, 2019, **119**, 7610–7672.

36 M. Konig, J. Vaes, E. Klemm and D. Pant, Solvents and supporting electrolytes in the electrocatalytic reduction of CO_2, *iScience*, 2019, **19**, 135–160.

37 W. Xi, R. Ma, H. Wang, Z. Gao, W. Zhang and Y. Zhao, Ultrathin ag nanowires electrode for electrochemical syngas production from carbon dioxide, *ACS Sustainable Chem. Eng.*, 2018, **6**, 7687–7694.

38 E. P. Delmo, Y. Wang, J. Wang, S. Zhu, T. Li, X. Qin, Y. Tian, Q. Zhao, J. Jang, Y. Wang, M. Gu, L. Zhang and M. Shao, Metal organic framework-ionic liquid hybrid catalysts for the selective electrochemical reduction of CO_2 to CH_4, *Chin. J. Catal.*, 2022, **43**, 1687–1696.

39 M. Sun, Z. Bian, W. Cui, X. Zhao, S. Dong, X. Ke, Y. Zhou and J. Wang, Pyrolyzing soft template-containing poly(ionic liquid) into hierarchical n-doped porous carbon for electroreduction of carbon dioxide, *Chin. J. Chem. Eng.*, 2022, **43**, 192–201.

40 H. Dong, M. Lu, Y. Wang, H. L. Tang, D. Wu, X. Sun and F. M. Zhang, Covalently anchoring covalent organic framework on carbon nanotubes for highly efficient electrocatalytic CO_2 reduction, *Appl. Catal., B*, 2022, **303**, 120897.

41 D. Faggion Jr., W. D. G. Goncalves and J. Dupont, CO_2 electroreduction in ionic liquids, *Front. Chem.*, 2019, **7**, 102.

42 J. J. Kaczur, H. Yang, Z. Liu, S. D. Sajjad and R. I. Masel, A review of the use of immobilized ionic liquids in the electrochemical conversion of CO_2, *Carbon*, 2020, **6**, 33.

43 S. Mena and G. Guirado, Electrochemical tuning of CO_2 reactivity in ionic liquids using different cathodes: From oxalate to carboxylation products, *Carbon*, 2020, **6**, 34.

44 X. Tan, X. Sun and B. Han, Ionic liquid-based electrolytes for CO_2 electroreduction and CO_2 electroorganic transformation, *Natl. Sci. Rev.*, 2022, **9**, nwab022.

45 K. K. Maniam and S. Paul, Ionic liquids and deep eutectic solvents for CO_2 conversion technologies-a review, *Materials*, 2021, **14**, 4519.

46 S. A. S. Mohammed, W. Z. N. Yahya, M. A. Bustam and M. G. Kibria, Elucidation of the roles of ionic liquid in CO_2 electrochemical reduction to value-added chemicals and fuels, *Molecules*, 2021, **26**, 6962.

47 Y. Huang, G. Cui, Y. Zhao, H. Wang, Z. Li, S. Dai and J. Wang, Preorganization and cooperation for highly efficient and reversible capture of low-concentration CO_2 by ionic liquids, *Angew. Chem., Int. Ed.*, 2017, **56**, 13293–13297.

48 Y. Huang, G. Cui, H. Wang, Z. Li and J. Wang, Tuning ionic liquids with imide-based anions for highly efficient CO_2 capture through enhanced cooperations, *J. CO2 Util.*, 2018, **28**, 299–305.

49 H. Wang, S. Zhang, J. Wang and Z. Yu, Standard partial molar volumes and viscosity B-coefficients of ionic liquids $[C_nmim]Br$ (n=4, 6, 8) in alcohols at 298.15k, *J. Mol. Liq.*, 2015, **209**, 563–568.

50 B. A. Rosen, A. Salehi-Khojin, M. R. Thorson, W. Zhu, D. T. Whipple, P. J. A. Kenis and R. I. Masel, Ionic liquid mediated selective conversion of CO_2 to CO at low overpotentials, *Science*, 2011, **334**, 643–644.

51 B. Kumar, M. Asadi, D. Pisasale, S. Sinha-Ray, B. A. Rosen, R. Haasch, J. Abiade, A. L. Yarin and A. Salehi-Khojin, Renewable and metal-free carbon nanofibre catalysts for carbon dioxide reduction, *Nat. Commun.*, 2013, **4**, 2819.

52 J. Choi, T. M. Benedetti, R. Jalili, A. Walker, G. G. Wallace and D. L. Officer, High performance Fe porphyrin/ionic liquid co-catalyst for electrochemical CO_2 reduction, *Chemistry*, 2016, **22**, 14158–14161.

53 Z. Min, B. Chang, C. Shao, X. Su, N. Wang, Z. Li, H. Wang, Y. Zhao, M. Fan and J. Wang, Enhancing CO_2 electroreduction to syngas by active protons of imidazolium ionic liquids: From performance to mechanism, *Appl. Catal.*, 2022, DOI: 10.1016/j.apcatb.2022.122185.

54 O. Kuntyi, G. Zozulya, M. Shepida and S. M. Soltani, CO_2 electroreduction in organic aprotic solvents: A mini review, *J. Chem.*, 2022, **2022**, 1–12.

55 S. Jin, Z. Hao, K. Zhang, Z. Yan and J. Chen, Advances and challenges for the electrochemical reduction of CO_2 to CO: From fundamentals to industrialization, *Angew. Chem., Int. Ed.*, 2021, **60**, 20627–20648.

56 X. Liu, B. Q. Li, B. Ni, L. Wang and H. J. Peng, A perspective on the electrocatalytic conversion of carbon dioxide to methanol with metallomacrocyclic catalysts, *J. Energy Chem.*, 2022, **64**, 263–275.

57 T. Shi, D. Sridhar, L. Zeng and A. Chen, Recent advances in catalyst design for the electrochemical and photoelectrochemical conversion of methane to value-added products, *Electrochem. Commun.*, 2022, **135**, 107220.

58 F. Chang, G. Zhan, Z. Wu, Y. Duan, S. Shi, S. Zeng, X. Zhang and S. Zhang, Technoeconomic analysis and process design for CO_2 electroreduction to co in ionic liquid electrolyte, *ACS Sustainable Chem. Eng.*, 2021, **9**, 9045–9052.

59 M. Rumayor, A. Dominguez-Ramos, P. Perez and A. Irabien, A techno-economic evaluation approach to the electrochemical reduction of CO_2 for formic acid manufacture, *J. CO2 Util.*, 2019, **34**, 490–499.

60 M. Jouny, W. Luc and F. Jiao, General techno-economic analysis of CO_2 electrolysis systems, *Ind. Eng. Chem. Res.*, 2018, **57**, 2165–2177.

61 D. Yang, Q. Zhu and B. Han, Electroreduction of CO_2 in ionic liquid-based electrolytes, *Innovation*, 2020, **1**, 100016.

62 S. Sharifi Golru and E. J. Biddinger, Effect of additives in aqueous electrolytes on CO_2 electroreduction, *Chem. Eng. J.*, 2022, **428**, 131303.

63 J. M. Vadillo, G. Diaz-Sainz, L. Gomez-Coma, A. Garea and A. Irabien, Chemical and physical ionic liquids in CO_2 capture system using membrane vacuum regeneration, *Membranes*, 2022, **12**, 785.

64 C. Ding, A. Li, S. M. Lu, H. Zhang and C. Li, In situ electrodeposited indium nanocrystals for efficient CO_2 reduction to CO with low overpotential, *ACS Catal.*, 2016, **6**, 6438–6443.

65 C. Du, P. Lu and N. Tsubaki, Efficient and new production methods of chemicals and liquid fuels by carbon monoxide hydrogenation, *ACS Omega*, 2020, **5**, 49–56.

66 G. P. Lau, M. Schreier, D. Vasilyev, R. Scopelliti, M. Gratzel and P. J. Dyson, New insights into the role of imidazolium-based promoters for the electroreduction of CO_2 on a silver electrode, *J. Am. Chem. Soc.*, 2016, **138**, 7820–7823.

67 F. Li, F. Mocci, X. Zhang, X. Ji and A. Laaksonen, Ionic liquids for CO_2 electrochemical reduction, *Chin. J. Chem. Eng.*, 2021, **31**, 75–93.

68 F. Liang, J. Zhang, Z. Hu, C. Ma, W. Ni, Y. Zhang and S. Zhang, Intrinsic defect-rich graphene coupled cobalt phthalocyanine for robust electrochemical reduction of carbon dioxide, *ACS Appl. Mater. Interfaces*, 2021, **13**, 25523–25532.

69 T. Oguma and K. Azumi, Improvement of electrochemical reduction of CO_2 using the potential-pulse polarization method, *Electrochemistry*, 2020, **88**, 451–456.

70 W. Guo, J. Bi, Q. Zhu, J. Ma, G. Yang, H. Wu, X. Sun and B. Han, Highly selective CO_2 electroreduction to CO on Cu–Co bimetallic catalysts, *ACS Sustainable Chem. Eng.*, 2020, **8**, 12561–12567.

71 R. Zhang, J. Yang, X. Zhao, H. Yang, H. Li, B. Ji, G. Zhou, X. Ma and D. Yang, Electrochemical deposited zeolitic imidazolate frameworks as an efficient electrocatalyst for CO_2 electrocatalytic reduction, *ChemCatChem*, 2022, **14**, e202101653.

72 T. Kunene, A. Atifi and J. Rosenthal, Selective CO_2 reduction over rose's metal in the presence of an imidazolium ionic liquid electrolyte, *ACS Appl. Energy Mater.*, 2019, **3**, 4193–4200.

73 I. Ganesh, BMIM-BF_4 RTIL: Synthesis, characterization and performance evaluation for electrochemical CO_2 reduction to CO over Sn and $MoSi_2$ cathodes, *Carbon*, 2020, **6**, 47.

© 2023 The Author(s). Co-published by the Institute of Process Engineering, Chinese Academy of Sciences and the Royal Society of Chemistry

Ind. Chem. Mater., 2023, **1**, 410–430 | **427**

74 S. Yu, A. J. Wilson, G. Kumari, X. Zhang and P. K. Jain, Opportunities and challenges of solar-energy-driven carbon dioxide to fuel conversion with plasmonic catalysts, *ACS Energy Lett.*, 2017, **2**, 2058–2070.

75 F. Ju, J. Zhang and W. Lu, Efficient electrochemical reduction of CO_2 to CO in ionic liquid/propylene carbonate electrolyte on ag electrode, *Catalysts*, 2020, **10**, 1102.

76 Y. Hu, J. Feng, X. Zhang, H. Gao, S. Jin, L. Liu and W. Shen, Efficient electrochemical reduction of CO_2 to CO in ionic liquids, *ChemistrySelect*, 2021, **6**, 9873–9879.

77 B. Ratschmeier and B. Braunschweig, Cations of ionic liquid electrolytes can act as a promoter for CO_2 electrocatalysis through reactive intermediates and electrostatic stabilization, *J. Phys. Chem. C*, 2021, **125**, 16498–16507.

78 H. Wang, D. Yang, J. Yang, X. Ma, H. Li, W. Dong, R. Zhang and C. Feng, Efficient electroreduction of CO_2 to CO on porous ZnO nanosheets with hydroxyl groups in ionic liquid-based electrolytes, *ChemCatChem*, 2021, **13**, 2570–2576.

79 A. V. Rudnev, K. Kiran and P. Broekmann, Specific cation adsorption: Exploring synergistic effects on CO_2 electroreduction in ionic liquids, *ChemElectroChem*, 2020, **7**, 1897–1903.

80 M. Zeng, Y. Liu, Y. Hu and X. Zhang, High-efficient CO_2 electrocatalysis over nanoporous Au film enabled by a combined pore engineering and ionic liquid-mediated approach, *Chem. Eng. J.*, 2021, **425**, 131663.

81 W. Guo, X. Tan, J. Bi, L. Xu, D. Yang, C. Chen, Q. Zhu, J. Ma, A. Tayal, J. Ma, Y. Huang, X. Sun, S. Liu and B. Han, Atomic indium catalysts for switching CO_2 electroreduction products from formate to CO, *J. Am. Chem. Soc.*, 2021, **143**, 6877–6885.

82 Y. Wu, C. Chen, X. Yan, X. Sun, Q. Zhu, P. Li, Y. Li, S. Liu, J. Ma, Y. Huang and B. Han, Boosting CO_2 electroreduction over a cadmium single-atom catalyst by tuning of the axial coordination structure, *Angew. Chem., Int. Ed.*, 2021, **60**, 20803–20810.

83 G. A. Olah, Beyond oil and gas: The methanol economy, *Angew. Chem., Int. Ed.*, 2005, **44**, 2636–2639.

84 X. Sun, Q. Zhu, X. Kang, H. Liu, Q. Qian, Z. Zhang and B. Han, Molybdenum-bismuth bimetallic chalcogenide nanosheets for highly efficient electrocatalytic reduction of carbon dioxide to methanol, *Angew. Chem., Int. Ed.*, 2016, **55**, 6771–6775.

85 D. X. Yang, Q. G. Zhu, C. J. Chen, H. Z. Liu, Z. M. Liu, Z. J. Zhao, X. Y. Zhang, S. J. Liu and B. X. Han, Selective electroreduction of carbon dioxide to methanol on copper selenide nanocatalysts, *Nat. Commun.*, 2019, **10**, 677.

86 L. Lu, X. Sun, J. Ma, D. Yang, H. Wu, B. Zhang, J. Zhang and B. Han, Highly efficient electroreduction of CO_2 to methanol on palladium-copper bimetallic aerogels, *Angew. Chem., Int. Ed.*, 2018, **57**, 14149–14153.

87 W. Guo, S. Liu, X. Tan, R. Wu, X. Yan, C. Chen, Q. Zhu, L. Zheng, J. Ma, J. Zhang, Y. Huang, X. Sun and B. Han, Highly efficient CO_2 electroreduction to methanol through atomically dispersed Sn coupled with defective CuO catalysts, *Angew. Chem., Int. Ed.*, 2021, **60**, 21979–21987.

88 P. Li, J. Bi, J. Liu, Q. Zhu, C. Chen, X. Sun, J. Zhang and B. Han, In situ dual doping for constructing efficient CO_2-to-methanol electrocatalysts, *Nat. Commun.*, 2022, **13**, 1965.

89 T. Sheng and S. G. Sun, Identifying the significance of proton-electron transfer in CH_4 production on Cu (100) in CO_2 electro-reduction, *J. Electroanal. Chem.*, 2017, **793**, 184–187.

90 H. Pan and C. J. Barile, Electrochemical CO_2 reduction to methane with remarkably high faradaic efficiency in the presence of a proton permeable membrane, *Energy Environ. Sci.*, 2020, **13**, 3567–3578.

91 S. Chen, B. Wang, J. Zhu, L. Wang, H. Ou, Z. Zhang, X. Liang, L. Zheng, L. Zhou, Y. Q. Su, D. Wang and Y. Li, Lewis acid site-promoted single-atomic Cu catalyzes electrochemical CO_2 methanation, *Nano Lett.*, 2021, **21**, 7325–7331.

92 Y. Wu, C. Chen, X. Yan, R. Wu, S. Liu, J. Ma, J. Zhang, Z. Liu, X. Xing, Z. Wu and B. Han, Enhancing CO_2 electroreduction to CH_4 over Cu nanoparticles supported on n-doped carbon, *Chem. Sci.*, 2022, **13**, 8388–8394.

93 Y. Wang, Z. Chen, P. Han, Y. Du, Z. Gu, X. Xu and G. Zheng, Single-atomic Cu with multiple oxygen vacancies on ceria for electrocatalytic CO_2 reduction to CH_4, *ACS Catal.*, 2018, **8**, 7113–7119.

94 X. Kang, Q. Zhu, X. Sun, J. Hu, J. Zhang, Z. Liu and B. Han, Highly efficient electrochemical reduction of CO_2 to CH_4 in an ionic liquid using a metal-organic framework cathode, *Chem. Sci.*, 2016, **7**, 266–273.

95 X. Sun, X. Kang, Q. Zhu, J. Ma, G. Yang, Z. Liu and B. Han, Very highly efficient reduction of CO_2 to CH_4 using metal-free n-doped carbon electrodes, *Chem. Sci.*, 2016, **7**, 2883–2887.

96 X. Liu, H. Yang, J. He, H. Liu, L. Song, L. Li and J. Luo, Highly active, durable ultrathin $MoTe_2$ layers for the electroreduction of CO_2 to CH_4, *Small*, 2018, **14**, e1704049.

97 L. Wang, Z. Luo, S. Feng, J. Ou, S. Luo, K. Yan and C. Wu, Synthesis of MOF-derived hybrids for efficient electrocatalytic reduction of CO_2 to syngas, *Catal. Lett.*, 2022, DOI: **10.1007/s10562-022-04089-x**.

98 R. Yun, B. Zhang, F. Zhan, Z. Xin, T. Sheng and Z. Shi, Electrocatalysis CO_2 to tunable syngas upon Fe clusters catalyst dispersed on bamboo-like NCT, *Inorg. Chem.*, 2022, **61**, 9375–9380.

99 J. Xiong, Syngas production via carbon dioxide electroreduction over Cds nanorods, *Int. J. Electrochem. Sci.*, 2021, **16**, 210369.

100 F. Marques Mota, D. L. T. Nguyen, J. E. Lee, H. Piao, J. H. Choy, Y. J. Hwang and D. H. Kim, Toward an effective control of the H_2 to CO ratio of syngas through CO_2 electroreduction over immobilized gold nanoparticles on layered titanate nanosheets, *ACS Catal.*, 2018, **8**, 4364–4374.

101 H. Xie, S. Chen, F. Ma, J. Liang, Z. Miao, T. Wang, H. L. Wang, Y. Huang and Q. Li, Boosting tunable syngas formation via electrochemical CO_2 reduction on Cu/In_2O_3 core/shell nanoparticles, *ACS Appl. Mater. Interfaces*, 2018, **10**, 36996–37004.

102 I. Hjorth, M. Nord, M. Rønning, J. Yang and D. Chen, Electrochemical reduction of CO_2 to synthesis gas on CNT supported $Cu_xZn_{1-x}O$ catalysts, *Catal. Today*, 2020, **357**, 311–321.

103 A. S. Varela, N. Ranjbar Sahraie, J. Steinberg, W. Ju, H. S. Oh and P. Strasser, Metal-doped nitrogenated carbon as an efficient catalyst for direct CO_2 electroreduction to CO and hydrocarbons, *Angew. Chem., Int. Ed.*, 2015, **54**, 10758–10762.

104 S. Y. Zhang, Y. Y. Yang, Y. Q. Zheng and H. L. Zhu, Ag-doped Co_3O_4 catalyst derived from heterometallic MOF for syngas production by electrocatalytic reduction of CO_2 in water, *J. Solid State Chem.*, 2018, **263**, 44–51.

105 N. Meng, C. Liu, Y. Liu, Y. Yu and B. Zhang, Efficient electrosynthesis of syngas with tunable CO/H_2 ratios over $Zn_x Cd_{1-x}$S-amine inorganic-organic hybrids, *Angew. Chem., Int. Ed.*, 2019, **58**, 18908–18912.

106 M. Beheshti, S. Kakooei, M. C. Ismail and S. Shahrestani, Investigation of CO_2 electrochemical reduction to syngas on Zn/Ni-based electrocatalysts using the cyclic voltammetry method, *Electrochim. Acta*, 2020, **341**, 135976.

107 A. Goeppert, M. Czaun, J. P. Jones, G. K. Surya Prakash and G. A. Olah, Recycling of carbon dioxide to methanol and derived products - closing the loop, *Chem. Soc. Rev.*, 2014, **43**, 7995–8048.

108 M. E. Dry, The fischer–tropsch process: 1950–2000, *Catal. Today*, 2002, **71**, 227–241.

109 P. C. Munasinghe and S. K. Khanal, Biomass-derived syngas fermentation into biofuels: Opportunities and challenges, *Bioresour. Technol.*, 2010, **101**, 5013–5022.

110 J. R. Rostrup-Nielsen, Syngas in perspective, *Catal. Today*, 2002, **71**, 243–247.

111 J. R. Rostrup-Nielsen, New aspects of syngas production and use, *Catal. Today*, 2000, **63**, 159–164.

112 J. Xu, X. Li, W. Liu, Y. Sun, Z. Ju, T. Yao, C. Wang, H. Ju, J. Zhu, S. Wei and Y. Xie, Carbon dioxide electroreduction into syngas boosted by a partially delocalized charge in molybdenum sulfide selenide alloy monolayers, *Angew. Chem., Int. Ed.*, 2017, **56**, 9121–9125.

113 C. Guan, J. Liu, C. Cheng, H. Li, X. Li, W. Zhou, H. Zhang and H. J. Fan, Hybrid structure of cobalt monoxide nanowire @ nickel hydroxidenitrate nanoflake aligned on nickel foam for high-rate supercapacitor, *Energy Environ. Sci.*, 2011, **4**, 4496–4499.

114 W. Zhu, Y. J. Zhang, H. Zhang, H. Lv, Q. Li, R. Michalsky, A. A. Peterson and S. Sun, Active and selective conversion of CO_2 to CO on ultrathin au nanowires, *J. Am. Chem. Soc.*, 2014, **136**, 16132–16135.

115 W. Metzger, R. Westfall, A. Hermann and P. Lyman, Nickel foam substrate for nickel metal hydride electrodes and lightweight honeycomb structures, *Int. J. Hydrogen Energy*, 1998, **23**, 1025–1029.

116 G. Yang, W. Xu, K. Tian, D. Su, J. Xu, H. Chen and Y. Zhang, Controllable syngas production on gold nanowires/nickel foam electrode in non-aqueous system, *J. Colloid Interface Sci.*, 2020, **579**, 290–296.

117 D. Yang, Q. Zhu, X. Sun, C. Chen, W. Guo, G. Yang and B. Han, Electrosynthesis of a defective indium selenide with 3D structure on a substrate for tunable CO_2 electroreduction to syngas, *Angew. Chem., Int. Ed.*, 2020, **59**, 2354–2359.

118 P. Qin, S. Yang, P. Zhan, M. Chu, G. Li, Z. Si, J. Shi, L. Lu, B. Han and T. Tan, Two-dimensional PdMo curved nanosheets for tunable CO_2 electrocatalytic reduction to syngas, *Cell Rep. Phys. Sci.*, 2021, **2**, 100619.

119 C. Q. Xi, J. K. Sang, A. Q. Wu, J. Yang, X. P. Qi, W. B. Guan, J. X. Wang and S. C. Singhal, Electrochemical performance and durability of flat-tube solid oxide electrolysis cells for H_2O/CO_2 co-electrolysis, *Int. J. Hydrogen Energy*, 2022, **47**, 10166–10174.

120 H. Y. Jeong, M. Balamurugan, V. S. K. Choutipalli, E. S. Jeong, V. Subramanian, U. K. Sim and K. T. Nam, Achieving highly efficient CO_2 to CO electroreduction exceeding 300 mA cm^{-2} with single-atom nickel electrocatalysts, *J. Mater. Chem. A*, 2019, **7**, 10651–10661.

121 Y. Huang, X. Zhang, X. Zhang, H. Dong and S. Zhang, Thermodynamic modeling and assessment of ionic liquid-based CO_2 capture processes, *Ind. Eng. Chem. Res.*, 2014, **53**, 11805–11817.

122 J. M. Spurgeon and B. Kumar, A comparative technoeconomic analysis of pathways for commercial electrochemical CO_2 reduction to liquid products, *Energy Environ. Sci.*, 2018, **11**, 1536–1551.

123 A. Paturska, M. Repele and G. Bazbauers, Economic assessment of biomethane supply system based on natural gas infrastructure, *Energy Procedia*, 2015, **72**, 71–78.

124 M. A. Adnan and M. G. Kibria, Comparative techno-economic and life-cycle assessment of power-to-methanol synthesis pathways, *Appl. Energy*, 2020, **278**, 115614.

125 Y. J. Guo, G. D. Li, J. B. Zhou and Y. Liu, Comparison between hydrogen production by alkaline water electrolysis and hydrogen production by pem electrolysis, *IOP Conf. Ser.: Earth Environ. Sci.*, 2019, **371**, 042022.

126 *G. C. B. 2021*, https://www.globalcarbonproject.org/, 2021, vol. 2022.

127 D. Steward, T. Ramsden and J. Zuboy, *H2A Central Hydrogen Production Model, Version 3 User Guide*, National Renewable Energy Laboratory, 2012.

128 J. Andersson, E. Furusjö, E. Wetterlund, J. Lundgren and I. Landälv, Co-gasification of black liquor and pyrolysis oil: Evaluation of blend ratios and methanol production capacities, *Energy Convers. Manage.*, 2016, **110**, 240–248.

129 S. Redl, S. Sukumara, T. Ploeger, L. Wu, T. Olshoj Jensen, A. T. Nielsen and H. Noorman, Thermodynamics and economic feasibility of acetone production from syngas using the thermophilic production host moorella thermoacetica, *Biotechnol. Biofuels*, 2017, **10**, 150.

130 V. Baghdjian, S. A. European methanol market mulls February contract price.

131 Methane price, https://www.globalpetrolprices.com/methane_prices/, 2022, [accessed 12 Sep. 2022].

132 Natural gas price, https://markets.businessinsider.com/commodities/natural-gas-price, 2022, [accessed 10 Oct. 2022].

© 2023 The Author(s). Co-published by the Institute of Process Engineering, Chinese Academy of Sciences and the Royal Society of Chemistry

Ind. Chem. Mater., 2023, **1**, 410–430 | **429**

133 Methanol price trend and forecast, https://www.chemanalyst.com/Pricing-data/methanol-1, 2022, [accessed 18 Oct. 2022].

134 S. Kibria Nabil, S. McCoy and M. G. Kibria, Comparative life cycle assessment of electrochemical upgrading of CO_2 to fuels and feedstocks, *Green Chem.*, 2021, **23**, 867–880.

135 B. Endrődi, G. Bencsik, F. Darvas, R. Jones, K. Rajeshwar and C. Janáky, Continuous-flow electroreduction of carbon dioxide, *Prog. Energy Combust. Sci.*, 2017, **62**, 133–154.

136 S. Verma, B. Kim, H. R. Jhong, S. Ma and P. J. Kenis, A gross-margin model for defining technoeconomic benchmarks in the electroreduction of CO_2, *ChemSusChem*, 2016, **9**, 1972–1979.

137 A. Sternberg, C. M. Jens and A. Bardow, Life cycle assessment of CO_2-based C1-chemicals, *Green Chem.*, 2017, **19**, 2244–2259.

138 T. T. H. Nguyen, T. Yamaki, S. Taniguchi, A. Endo and S. Kataoka, Integrating life cycle assessment for design and optimization of methanol production from combining methane dry reforming and partial oxidation, *J. Cleaner Prod.*, 2021, **292**, 125970.

139 A. Sternberg and A. Bardow, Life cycle assessment of power-to-gas: Syngas vs methane, *ACS Sustainable Chem. Eng.*, 2016, **4**, 4156–4165.

140 R. Farahipour and A. T. Karunanithi, Life cycle environmental implications of CO_2 capture and sequestration with ionic liquid 1-butyl-3-methylimidazolium acetate, *ACS Sustainable Chem. Eng.*, 2014, **2**, 2495–2500.

141 J. Artz, T. E. Müller, K. Thenert, J. Kleinekorte, R. Meys, A. Sternberg, A. Bardow and W. Leitner, Sustainable conversion of carbon dioxide: An integrated review of catalysis and life cycle assessment, *Chem. Rev.*, 2017, **118**, 434–504.

142 A. S. Miriam Werder, Life cycle assessment of the conventional and solar thermal production of zinc and synthesis gas, *Energy*, 2000, **25**, 395–409.

143 D. Xu, K. Li, B. Jia, W. Sun, W. Zhang, X. Liu and T. Ma, Electrocatalytic CO_2 reduction towards industrial applications, *Carbon Energy*, 2023, **5**(1), DOI: 10.1002/cey2.230.

144 Z. Duan, R. Sun, C. Zhu and I. M. Chou, An improved model for the calculation of CO_2 solubility in aqueous solutions containing Na^+, K^+, Ca^{2+}, Mg^{2+}, Cl^-, and SO_4^{2-}, *Mar. Chem.*, 2006, **98**, 131–139.

145 S. Kaneco, K. Iiba, H. Katsumata, T. Suzuki and K. Ohta, Effect of sodium cation on the electrochemical reduction of CO_2 at a copper electrode in methanol, *J. Solid State Electrochem.*, 2006, **11**, 490–495.

146 F. Zhang, H. Zhang and Z. Liu, Recent advances in electrochemical reduction of CO_2, *Curr. Opin. Green Sustainable Chem.*, 2019, **16**, 77–84.

147 Acetonitrile Price Trend and Forecast, https://www.chemanalyst.com/Pricing-data/acetonitrile-1105, 2022, [accessed 15 Oct. 2022].

148 Dimethylformamide Price Trend and Forecast, https://www.chemanalyst.com/Pricing-data/dimethylformamide-dmf-1167, 2022, [accessed 15 Oct. 2022].

149 Eu sodium carbonate market report: Consumption, suppliers, buyers and forecast – indexbox, https://www.Globenewswire.Com/en/news-release/2022/06/08/2458413/0/en/eu-sodium-carbonate-market-report-consumption-suppliers-buyers-and-forecast-indexbox.Html, 2021, [accessed 14 jan. 2023].

150 L. Yuan, L. Zhang, J. Feng, C. Jiang, J. Feng, C. Li, S. Zeng and X. Zhang, Upscaling studies for efficiently electric-driven CO_2 reduction to CO in ionic liquid-based electrolytes, *Chem. Eng. J.*, 2022, **450**, 138378.

151 S. P. F. Costa, A. M. O. Azevedo, P. Pinto and M. Saraiva, Environmental impact of ionic liquids: Recent advances in (eco)toxicology and (bio)degradability, *ChemSusChem*, 2017, **10**, 2321–2347.

152 M. Bystrzanowska, F. Pena-Pereira, L. Marcinkowski and M. Tobiszewski, How green are ionic liquids? - a multicriteria decision analysis approach, *Ecotoxicol. Environ. Saf.*, 2019, **174**, 455–458.

153 N. Adhikari and D. R. Joshi, An overview on common organic solvents and their toxicity, *Int. J. Pharm.*, 2019, **28**, 1–18.